Computational and Structural Biotechnology Journal 18 (2020) 1509–1524

ELSEVIER

COMPUTATIONAL ANDSTRUCTURAL BIOTECHNOLOGY JOURNAL

journal homepage: www.elsevier.com/locate/csbj

Comparison of unsupervised machine-learning methods to identify metabolomic signatures in patients with localized breast cancer

Jocelyn Gal [a,1,*], Caroline Bailleux [b,1], David Chardin [c,d,1], Thierry Pourcher [d], Julia Gilhodes [e], Lun Jing [d], Jean-Marie Guigonis [d], Jean-Marc Ferrero [b], Gerard Milano [f], Baharia Mograbi [g], Patrick Brest [g], Yann Chateau [a], Olivier Humbert [c,d], Emmanuel Chamorey [a]

[a] University Côte d'Azur, Epidemiology and Biostatistics Department, Centre Antoine Lacassagne, Nice F-06189, France
[b] University Côte d'Azur, Medical Oncology Department Centre Antoine Lacassagne, Nice F-06189, France
[c] University Côte d'Azur, Nuclear Medicine Department, Centre Antoine Lacassagne, Nice F-06189, France
[d] University Côte d'Azur, Commissariat à l'Energie Atomique, Institut de Biosciences et Biotechnologies d'Aix-Marseille, Laboratory Transporters in Imaging and Radiotherapy in Oncology, Faculty of Medicine, Nice F-06100, France
[e] Department of Biostatistics, Institut Claudius Regaud, IUCT-O Toulouse, France
[f] University Côte d'Azur, Centre Antoine Lacassagne, Oncopharmacology Unit, Nice F-06189, France
[g] University Côte d'Azur, CNRS UMR7284, INSERM U1081, IRCAN TEAM4 Centre Antoine Lacassagne FHU-Oncoage, Nice F-06189, France

ARTICLE INFO

Article history:
Received 11 February 2020
Received in revised form 15 May 2020
Accepted 16 May 2020
Available online 3 June 2020

Keywords:
Unsupervised machine learning
Metabolomics
Breast neoplasms
Computer simulation

ABSTRACT

Genomics and transcriptomics have led to the widely-used molecular classification of breast cancer (BC). However, heterogeneous biological behaviors persist within breast cancer subtypes. Metabolomics is a rapidly-expanding field of study dedicated to cellular metabolisms affected by the environment. The aim of this study was to compare metabolomic signatures of BC obtained by 5 different unsupervised machine learning (ML) methods. Fifty-two consecutive patients with BC with an indication for adjuvant chemotherapy between 2013 and 2016 were retrospectively included. We performed metabolomic profiling of tumor resection samples using liquid chromatography-mass spectrometry. Here, four hundred and forty-nine identified metabolites were selected for further analysis. Clusters obtained using 5 unsupervised ML methods (PCA k-means, sparse k-means, spectral clustering, SIMLR and k-sparse) were compared in terms of clinical and biological characteristics. With an optimal partitioning parameter k = 3, the five methods identified three prognosis groups of patients (favorable, intermediate, unfavorable) with different clinical and biological profiles. SIMLR and K-sparse methods were the most effective techniques in terms of clustering. *In-silico* survival analysis revealed a significant difference for 5-year predicted OS between the 3 clusters. Further pathway analysis using the 449 selected metabolites showed significant differences in amino acid and glucose metabolism between BC histologic subtypes. Our results provide proof-of-concept for the use of unsupervised ML metabolomics enabling stratification and personalized management of BC patients. The design of novel computational methods incorporating ML and bioinformatics techniques should make available tools particularly suited to improving the outcome of cancer treatment and reducing cancer-related mortalities.

1. Introduction

Breast cancer (BC) is the most common type of cancer in women worldwide and the second leading cause of cancer-associated deaths [1]. The treatment strategy may be guided by two classifications indicating the aggressiveness of the tumor. The anatomy-clinical classification is based on age, TNM, histological factors (histological grade, Ki-67) as well as on hormonal-receptor status and Her-2 expression. The molecular classification resulting from genomic [2], transcriptomic [3] and proteomic [4] analyses introduced the concept of luminal A, luminal B, Her-2 and basal-like BC [5–7]. This latter classification from Perou and Sorlie was assessed using unsupervised analyses [6,8]. Efforts have been made to develop multivariate prognostic models such as, AdjuvantOnline®,

* Corresponding author at: Department of Epidemiology and Biostatistics, Centre Antoine Lacassagne, University Côte d', Azur 33 avenue de Valombrose, 06189 Nice, France.

E-mail address: jocelyn.gal@nice.unicancer.fr (J. Gal).

[1] These authors contributed equally to this work.

https://doi.org/10.1016/j.csbj.2020.05.021
2001-0370/© 2020 The Authors. Published by Elsevier B.V. on behalf of Research Network of Computational and Structural Biotechnology.

PREDICT Tool [9,10] and multigene predictors [11,12]. The use of biomarker-based tests, including omics-based tests, has steadily increased over the last decade as a result of the need for personalized treatment strategies designed to optimize outcomes [13–18]. Several genomic prognostic markers have been described for BC such as OncotypeDX®, Prosigna®, MammaPrint®, Endopredict® Genomic grade index® and BC Index® [19]. Two markers are commercially available and are increasingly used in clinical practice (21-gene recurrence score OncotypeDX® and 70-gene prognostic signature MammaPrint®). However, heterogeneity persists in biological features within BC subtypes, thus highlighting the need to improve the taxonomy [20]. This heterogeneity may be related to specific combinations of genetic, pathological and environmental factors leading to specific metabolic alterations and interactions [21,22].

Metabolomics is a new and growing field dedicated to the study of metabolism at overall level that promises to provide new insights into disease mechanisms and drug effects. Indeed, metabolomics may offer a complementary approach to genomics and could be used to better understand the influence of the environment on tumor phenotype [23]. Two distinct approaches characterize metabolomics: a targeted approach aimed at quantifying as accurately as possible a limited number of predefined metabolites of interest [24] and an untargeted approach aimed at measuring, without any a priori, as many metabolites as possible in a sample [25,26]. As with other omics approaches, metabolomics generates high-dimensional data. The processing of these data can be done by applying supervised or unsupervised machine learning (ML) algorithms that are increasingly used for medical diagnosis and therapeutic strategy guidance [27–29]. Unsupervised ML, in which no a priori class label information is given to guide the algorithm [30], seems a suitable alternative to analyze these data and address the problem of BC heterogeneity [6]. The aim of this study was to compare metabolomic signatures of BC obtained using five different unsupervised ML methods. To evaluate the consistency of our results, the clusters obtained by unsupervised ML methods were compared with patients' clinical characteristics and identified metabolic pathways.

2. Material and methods

2.1. Patients

This is a retrospective cohort study based on data and samples from 52 patients already available in the Centre Antoine Lacassagne tumor bank and collected during routine practice between 2013 and 2016. Patient tumor characteristics were: clinical stages I to III$_B$ biopsy-proven BC, with an indication for post-surgery adjuvant therapy. Tumor phenotypes were classified into three subtypes: triple-negative (estrogen receptor, progesterone receptor and Her-2 non-over-expressed); luminal (estrogen receptor and/or progesterone receptor positive and Her-2 non-over-expressed); Her-2 over-expressed (Her-2 over-expressed, estrogen receptor and progesterone receptor either positive or negative) [31]. After surgery, all patients were treated according to current guidelines, with sequential chemotherapy including anthracyclines (epirubicin and cyclophosphamide) and taxanes followed by radiotherapy. Patients with Her-2 over-expressed tumors were treated with trastuzumab concurrently with taxanes and continued for one year. Patients with luminal BC were then treated by endocrine therapy with tamoxifen or an aromatase inhibitor, based on menopausal status. Clinical, histological, radiological and therapeutic data were retrospectively extracted from our facility's digital records or collected by a clinical data monitor. Follow-up data were either extracted from our facility's digital records or retrieved by telephone if patients had changed facilities during surveillance. Written informed consent was obtained from all study participants. All procedures performed in this study involving tissue collection and analyses were following the ethical standards of the institutional and/or national research committee (French National Commission for Informatics and Liberties N°17003 and National Institute Health data N°1515251018).

2.2. Data-preprocessing, metabolite identification, statistical and pathway analysis

Sample collection, preparation and data-processing using MZmine [32,33] are shown in Supplementary Material S1 and Supplementary Fig. 1 Metabolites obtained from positive and negative ionization modes were combined. Only metabolites with no null values after pre-processing were selected for analysis. When a metabolite was detected in both positive and negative modes, only the mode offering the highest average intensity was considered. After these steps, 1271 metabolites were identified. To eliminate noisy data, a filtering function was applied before statistical analysis. Finally, statistical analysis was performed on 449 metabolites. The identification of metabolic pathways was performed using MetaboAnalyst database sources [34]. The impact score was determined by the relative pathway topological effect of the metabolites, and -log*(p)* was used as the enrichment score, reflecting the probability of the pathway being identified at random; the number of "hits" was the actual number of matched metabolites in the pathway. For the selection of the most relevant pathways, we applied the following criteria: Impact >0, FDR < 0.25 and p < 0.05 [35].

A Venn diagram (http://bioinformatics.psb.ugent.be/webtools/Venn/) was used to display all possible logical relations between the metabolites or pathways identified by the clustering methods. Differences between clusters regarding the most active metabolites were plotted using boxplots.

2.3. Clustering algorithms

Five unsupervised clustering methods were selected and compared: Principal Component Analysis (PCA) k-means, Sparse k-means, Single-cell Interpretation via Multi-kernel LeaRning (SIMLR), k-sparse and Spectral clustering. Many clustering approaches exist, among which two of the most popular are K-means and spectral clustering [36]. PCA k-means and Sparse k-means are two well established, K-means based methods frequently used in computational. SIMLR and K-sparse are two recently developed k-means based methods of particular interest for omics data. These methods use different dimension reduction steps with k-means. In order to apply these five unsupervised clustering methods, the optimal number of clusters was determined in advance using five criteria: gap [37], silhouette [38,39], Davies-Bouldin [40], Calinski-Harabasz [41] and SIMLR method [42]. PCA k-means clustering, combines PCA to reduce the number of dimensions of a dataset and the k-means method to minimize the intra-cluster variance for a chosen number of k clusters [43–45]. Spectral clustering [46,47] is based on graph theory. It consists of identifying dense regions in a multidimensional dataset, i.e. observations that can form a non-convex set but are close to each other. Sparse k-means clustering was developed in 2010 by Witten and Tibshirani [8]. This method is based on a Least Absolute Shrinkage and Selection Operator (LASSO) approach [48] and combines the LASSO approach and the k-means method which simultaneously find the clusters and select features. SIMLR clustering [42] was developed to analyze scRNA-seq data. This method searches for appropriate cell-to-cell similarity metrics to perform dimension reduction and clustering. In multiple-kernel learning frameworks, this method may be especially beneficial for data containing no identifiable clusters. K-sparse clustering [49] is an algorithm combining dimension reduction and relevant feature selection using a constraint in L1-norm rather than a lasso-type penalty to select the features. The performance of an unsupervised clustering method is measured by its ability to partition data. Partitioning is considered optimal when it minimizes the average distance between patients within a cluster (homogeneity) and maximizes cluster distances 2 by 2 (separability). The performances of the five methods were compared using the silhouettes index (SI) [39]. The SI ranges between -1 and 1 and assesses whether a patient belongs to the "right" cluster. The closer the index is to 1, the more satisfactory the assignment of a patient to a cluster. The t-SNE method was used for data visualization [50]. Processing times were obtained on a computer using an i5 processor (3.1 GHz).

2.4. Clinical evaluation

The relevance of the discovered clusters was assessed by comparing the clinical and survival characteristics between clusters using χ^2 or Fisher's exact tests for categorical data, analysis of variance or Mann-Whitney's test for continuous variables and log-rank test for censored data. Overall survival (OS) was defined as the time between diagnosis and death due to any cause. Specific survival (SS) was determined by the time between diagnosis and death due to BC. Recurrence-Free Survival (RFS) was defined as the time between diagnosis and the first recurrence (local, regional and metastasis). Patients showing no event (death or recurrence) or lost to follow-up were censored at the date of their last contact. OS, SS, and RFS were estimated using the Kaplan-Meier method. Median follow-up with a 95% confidence interval was calculated by reverse Kaplan–Meier method. All analyses were performed with Matlab® R2018b for PCA k-means, Spectral clustering, SIMLR (https://github.com/BatzoglouLabSU/SIMLR/tree/SIMLR/MATLAB) and k-sparse clustering and R [51] using package Sparcl [52] for sparse k-means clustering. The difference between clusters regarding the most biologically significant metabolites was plotted using boxplots. For clinical and biological analyses, all p-values <0.05 (two-sided) were considered statistically significant.

2.5. Prediction for 5- and 10-year overall and specific survival

Web-based prognostication PREDICT tool (https://breast.predict.nhs.uk/tool) [9,10,53] was used to estimate predicted OS (pOS) and predicted SS (pSS) at 5 and 10 years, based on several patient and tumor characteristics. For each patient, ten characteristics were entered manually: age at diagnosis, menopausal status, estrogen receptor status, Her-2 status, Ki-67 status, tumor stage, histological grade, mode of detection, number of positive nodes and presence of micrometastases. PREDICT tool can be used to estimate expected overall survival at 5 years and 10 years in the absence of available survival data due to short follow-up. If information was missing for detection, bisphosphonate therapy or menopausal status, patients were not excluded but the "unknown" category was used. Only one patient was excluded because of missing tumor grade data. A 1000 resamples bootstrap was used to estimate the 95% confidence interval.

3. Results

3.1. Patient characteristics

Tumor and treatment features of the 52 patients were described in Table 1. Median age was 63 years (range: 37–88). The main histological type was invasive ductal carcinoma (92%), and the main tumor stages were T1 (40.5%) and T2 (46%). Twenty-four patients (46%) presented axillary lymph node invasion. Two patients (4%) were oligometastatic at diagnosis. Forty-three percent of patients had histological grade II tumors and 47% had grade III tumors. Half of the patients had negative hormone receptor status (48%) and 24% of patients had Her-2 over-expression. Median follow-up was 48.5 months (95%CI [43–54.5]). Twenty-one patients presented a recurrence: 4 local recurrences (7.5%), 6 regional recurrences (11.5%) and 11 metastatic recurrences (21%). Three-year OS was 90% [82–99], 3-year SS was 92% [85–100] and 3-year RFS was 82% [72–93] (Supplementary Fig. 2). Median OS, SS, and RFS were not reached.

Table 1
Patients' demographics and treatment characteristics.

Clinical characteristic	No. of patients	%
Age (median min – max)	63.2 (37–88)	
Histology type		
Invasive ductal carcinoma	48	92
Invasive lobular carcinoma	3	6
Microinvasive carcinoma	1	2
Tumor stage		
T1	21	40.5
T2	24	46
T3	7	13.5
Axillary lymph node status		
N0	28	54
N+	24	46
Metastasis		
M0	50	96
M1	2	4
Histological grade		
I	5	10
II	22	43
III	24	47
Hormonal receptors status*		
Negative	25	48
Positive	27	52
Her-2 status		
Non-over-expressed	40	74
Over-expressed	12	24
Triple-negative status		
No	37	71
Yes	15	29
Tumor phenotype		
Her2	12	23
Luminal	25	48
Triple-Negative	15	29
Adjuvant Chemotherapy		
No	13	25
Yes	39	75
Adjuvant Radiotherapy		
No	9	17
Yes	43	83
Adjuvant Hormonotherapy		
No	24	46
Yes	28	54

* Oestrogen and/or progesterone.

3.2. Clustering results

3.2.1. Estimated number of clusters

Using four methods (Gap statistic, Calinski-Harabasz, Silhouette and SIMLR criterion), the optimal number of clusters was equal to three (k = 3) (Supplementary Fig. 3). Only for Davies-Bouldin criterion, the optimal number of clusters was equal to four (k = 4). It seems reasonable, therefore, to conclude that the optimal number of clusters is equal to 3.

3.2.2. Patient distribution

Three clusters were identified with each of the five clustering methods, (Fig. 1). In terms of processing times, PCA k-means was the fastest and K-sparse was the longest (Supplementary Table 1). SIMLR and k-sparse methods were the most discriminants with an average silhouette value of 0.85 and 0.91, respectively (Fig. 2). Seventy-three percent of patients (38/52) were ranked in the same clusters by the five methods, 17.5% of patients (9/52) were classified in the same clusters by 4 methods and 9.5% of patients (5/52) were classified in the same clusters by 3 methods.

3.2.3. Comparison of clinical characteristics between clusters

As shown in Table 2, the 5 methods revealed significant inter-cluster differences. Patients in cluster 3 had mainly unfavorable prognostic factors: tumor stage T2/T3, histological grade III, high mitotic score and triple-negative phenotype. In contrast, patients in cluster 1 had mainly favorable prognosis factors: tumor stage T1, histological grade I/II, lower mitotic score and luminal phenotype, whereas patients in cluster 2 constitute an intermediate group presenting both good and poor prognostic factors. Clusters defined by PCA k-means were significantly different for 5 characteristics: tumor stage, mitosis, tumor phenotype, Her-2 status and luminal. Clusters defined by Spectral Clustering were significantly different for 6 characteristics: tumor stage, histological grade, mitosis, Ki67, tumor phenotype and luminal. Clusters defined by Sparse k-means were significantly different for 4 characteristics: histological grade, tumor phenotype, Her-2 status and luminal. Clusters defined by SIMLR were significantly different for 6 characteristics: tumor stage, histological grade, mitosis, Ki67, tumor phenotype and luminal. Clusters defined by K-Sparse were significantly different for 6 characteristics: tumor stage, histological grade, mitosis, Ki67, tumor phenotype and luminal. From a strictly clinical point of view, Spectral clustering, SIMLR and K-sparse are the 3 most discriminating methods. Indeed, for these 3 methods, six prognostic factors (tumor stage, histological grade, mitosis score, Ki-67, tumor phenotype and luminal) were distributed significantly different between the 3 clusters.

3.2.4. Comparison of survival and predicted survival between clusters

None of the methods created clusters showing significant differences for OS, SS or RFS. Analysis of patients' simulated survival data

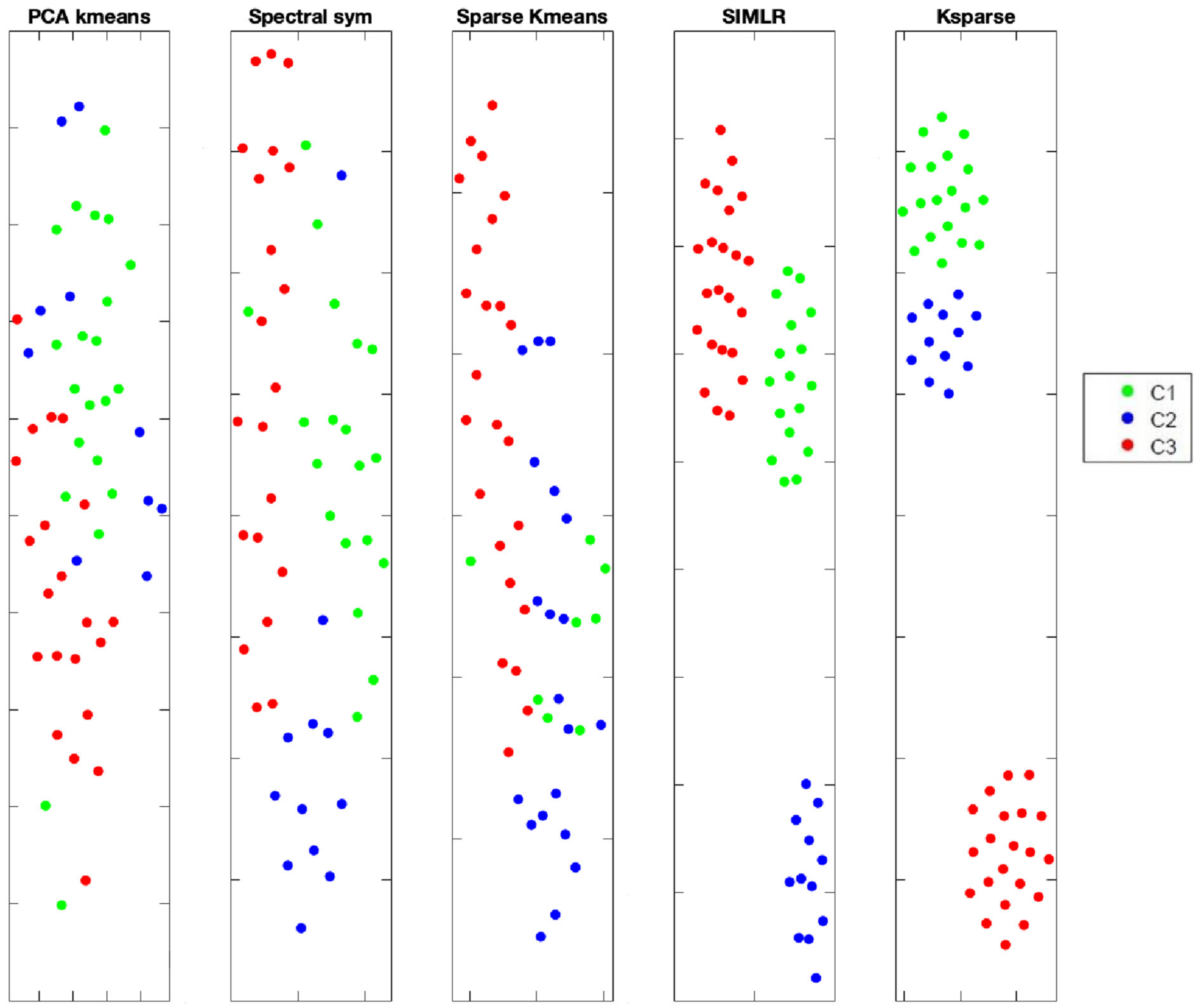

Cluster 1: Patients are represented in green
Cluster 2: Patients are represented in blue
Cluster 3: Patients are represented in red

Fig. 1. Visualization of each cluster by clustering method using T-sne.

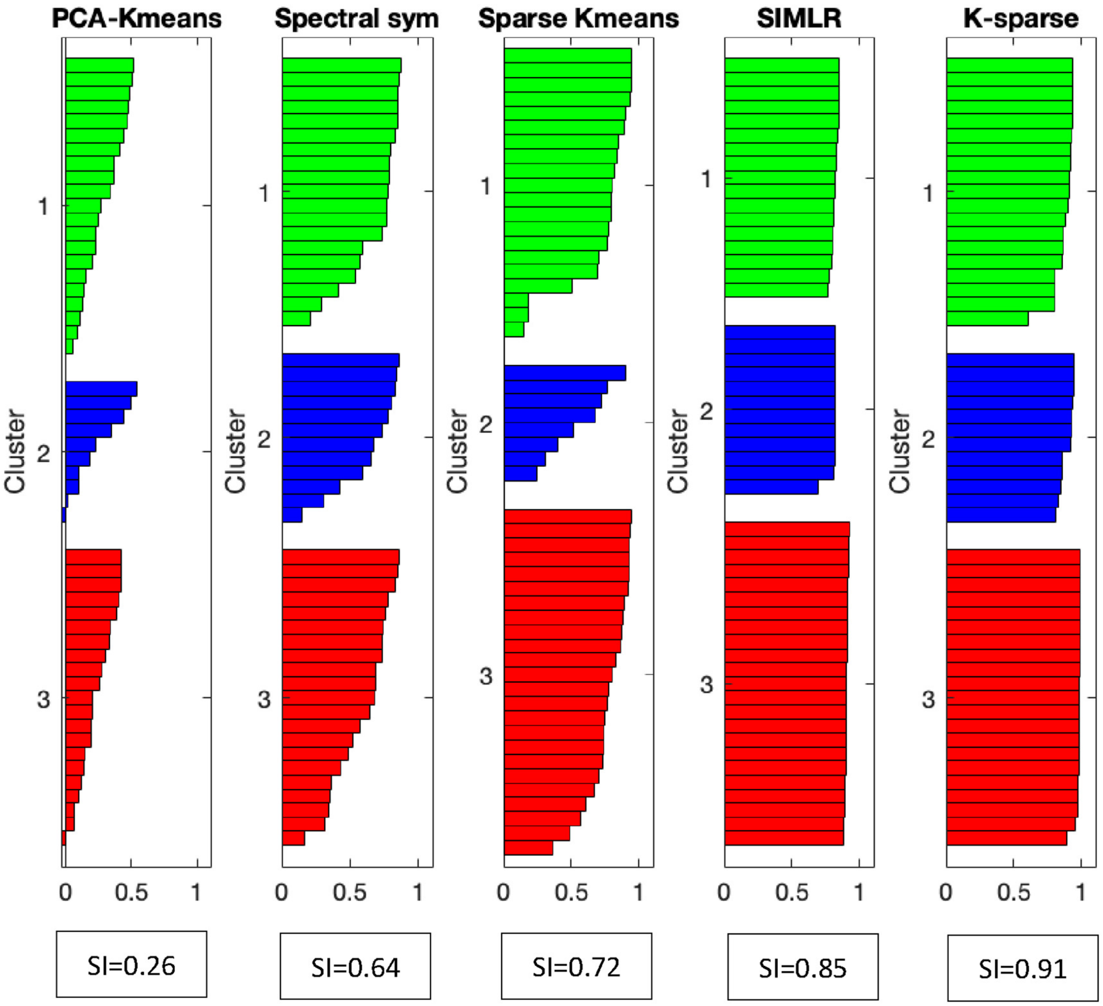

Fig. 2. Silhouette value (SI) representation for each patient by clustering method.

using PREDICT tool are presented in Table 3 and show a predicted survival gradient for clusters obtained with the 5 methods for OS and SS. There were significant differences for 5-year pOS between clusters obtained with K-sparse (p = 0.021), Sparse K-means (p = 0.049), Spectral and clustering (p = 0.021). The five methods showed a significant difference for 5-year pSS between clusters. In terms of 10-year pOS, there were no significant differences between clusters obtained by any of the 5 methods. In contrast, for 10-year pSS, the 5 methods showed significant differences between clusters. Patients in cluster 3 clearly showed the poorest predicted survival.

3.2.5. Comparison of the most impactful metabolites according to the five methods

To relate the impact of 449 metabolites to cluster construction, we ranked these metabolites extracted from each of the five methods based on their functional contributions to outputs. With this approach, we classified the relative impact of metabolites on cluster construction and on the identification of metabolic signatures. The highest-ranked metabolites were those that provided relevant information to the signature versus those that provided redundant information or no information. Among a total of 449 metabolites, 116 (26%) were selected by K-sparse clustering and 69 (15%) by Sparse K-means clustering. As for the three other methods, which don't select sparse features, the number of metabolites remained equal to 449. The 50 most effective metabolites identified by the five methods are presented in Supplementary Table 2. Furthermore, a comparison of the top 50 metabolites in each of the 5 methods is presented using a Venn diagram (Fig. 3). Two metabolites were shared by the 5 methods (Creatine, L-Proline), 9 were shared by 4 methods (Betaine, Glutathione, Humulinic Acid A, Isoleucyl-Methionine, L-Carnitine, L-Methionine, L-Phenylalanine Triethanolamine, Alnustone), 28 were shared by 3 methods and 38 were shared by 2 methods (Table 4).

3.2.6. Comparison between 5 methods of identified metabolic pathways

For a better understanding of metabolic dysregulation among BC subtypes, pathway analysis was performed. Identification of all the metabolic pathways highlighted by each of the 5 methods as shown in Supplementary Table 3. The most relevant pathways for each of the 5 methods are shown in Table 5. Sparse K-means identified only one statistically significant pathways, "cysteine and methionine metabolism", involved in amino acid metabolism. K-Sparse identified 3 different pathways: "glycerolipid metabolism", "Starch and sucrose metabolism" involved in carbohydrates metabolic pathway and "Aminoacyl-tRNA biosynthesis" involved in translation pathway. Spectral clustering identified 17 pathways, the 3 most important being "Glycine, serine and threonine metabolism", "Alanine, aspartate and glutamate metabolism" and "Histidine metabolism and glutathione metabolism" involved in amino acid metabolic pathway. PCA K-

Table 2
Clinical comparison of 52 patients between clusters.

Clinical characteristic	PCA-K-means				Spectral Clustering				Sparse K-means				SIMLR				K-Sparse			
	C1 (N = 21)	C2 (N = 10)	C3 (N = 21)	P-value	C2 (N = 19)	C1 (N = 12)	C3 (N = 21)	P-value	C1 (N = 24)	C2 (N = 8)	C3 (N = 20)	P-value	C1 (N = 17)	C2 (N = 12)	C3 (N = 23)	P-value	C1 (N = 19)	C2 (N = 12)	C3 (N = 21)	P-value
Age [a]	62.7 (15.2)	64.8(16)	62.9(15)	0.93	64.8 (14.3)	62.5 (16.5)	62 (15.3)	0.8	64.1(15)	60.5 (17.2)	63 (14.9)	0.85	64.3 (14.1)	64.9 (16.1)	61.4 (15.6)	0.755	64.8 (14.3)	62.5 (16.5)	62(15.3)	0.827
Histology type				1				0.392				0.106				0.752				0.392
Ductal carcinoma	19(90.5)	10(1 0 0)	19(90.5)		17(89.5)	11(91.7)	20(95.2)		21(87.5)	7(87.5)	20(1 0 0)		15(88.2)	12(1 0 0)	21(91.3)		17(89.5)	11(91.7)	20(95.2)	
Lobular carcinoma	2(9.5)	0(0)	1(4.8)		2(10.5)	1(8.3)	0(0)		3(12.5)	0(0)	0(0)		2(11.8)	0(0)	1(4.3)		2(10.5)	1(8.3)	0(0)	
Microinvasive carcinoma	0(0)	0(0)	1(4.8)		0(0)	0(0)	1(4.8)		0(0)	1(12.5)	0(0)		0(0)	0(0)	1(4.3)		0(0)	0(0)	1(4.8)	
Tumor stage				0.005				**0.018**				0.063				**0.045**				**0.018**
T1	14(66.7)	3(30)	4(19)		12(63.2)	5(41.7)	4(19)		14(58.3)	2(25)	5(25)		10(58.8)	6(50)	5(21.7)		12(63.2)	5(41.7)	4(19)	
T2/T3	7(33.3)	7(70)	17(81)		7(36.8)	7(58.3)	17(81)		10(41.7)	6(75)	15(75)		7(41.2)	6(50)	18(78.3)		7(36.8)	7(58.3)	17(81)	
Axillary lymph node				0.162				0.075				0.526				0.387				0.075
N0	14(66.7)	6(60)	8(38.1)		14(73.7)	6(50)	8(38.1)		15(62.5)	4(50)	9(45)		11(64.7)	7(58.3)	10(43.5)		14(73.7)	6(50)	8(38.1)	
N+	7(33.3)	4(40)	13(61.9)		5(26.3)	6(50)	13(61.9)		9(37.5)	4(50)	11(55)		6(35.3)	5(41.7)	13(56.5)		5(26.3)	6(50)	13(61.9)	
Metastasis				0.667				1				1				0.497				1
M0	21(1 0 0)	10(1 0 0)	19(90.5)		18(94.7)	12(1 0 0)	20(95.2)		23(96)	8(1 0 0)	19(95)		17(1 0 0)	12(1 0 0)	21(86.9)		18(94.7)	12(1 0 0)	20(95.2)	
M1	0(40)	0(0)	2(9.5)		1(5.3)	0(0%)	1(4.8)		1(4)	0(0%)	1(5)		0(0%)	0(0%)	2(13.1)		1(5.3)	0(0)	1(50)	
Histological grade				0.109				**0.025**				**0.008**				**0.007**				**0.025**
I/II	13(61.9)	7(70)	7(35)		12(63.2)	9(75)	6(30)		15(62.5)	5(71.4)	7(35)		11(64.7)	9(75)	7(31.8)		12(63.2)	9(75)	6(30)	
III	8(38.1)	3(30)	13(75)		7(36.8)	3(25)	14(70)		9(37.5)	2(28.6)	13(65)		6(35.3)	3(25)	15(68.2)		7(36.8)	3(25)	14(70)	
Mitosis				**0.024**				**0.016**				0.133				**0.005**				**0.016**
1	11(52.4)	4(40)	2(10)		10 (52.6)	5 (41.7)	2 (10)		11 (45.8)	2 (28.6)	4 (20)		10 (58.8)	5 (41.7)	2 (9.1)		10 (52.6)	5 (41.7)	2 (10)	
2	3(14.3)	4(40)	7(35)		3 (15.8)	5 (41.7)	6 (30)		4 (16.7)	4 (57.1)	6 (30)		2 (11.8)	5 (41.7)	7 (31.8)		3 (15.8)	5 (41.7)	6 (30)	
3	7(33.3)	2(20)	11(55)		6 (31.6)	2 (16.7)	10 (60)		9 (37.5)	1 (14.3)	10 (50)		5 (29.4)	2 (16.7)	13 (59.1)		6 (31.6)	2 (16.7)	12 (60)	
Ki67 [a]	25 (5,100)	27.5 (10,90)	60 (10,90)	0.066	41.1 (30.6)	33(22.6)	58.8 (27.2)	**0.027**	30 (19.2, 80)	35 (23.8, 45)	60 (28.8, 90)	0.196	38 (31)	32.8 (22.7)	59.7 (25.9)	**0.009**	41.1 (30.6)	33 (22.6)	58.8 (27.2)	**0.027**
Tumour phenotype				**0.024**				**0.012**				**0.006**				**0.018**				**0.012**
Her-2 over-expressed	1(4.8)	4(40)	7(33.3)		1(5.3)	4(33.3)	7(33.3)		2(8.3)	4(50)	6(30)		1(5.9)	4(33.3)	7(30.4)		1(5.3)	4(33.3)	7(33.3)	
Luminal	14(66.7)	5(50)	6(28.6)		13(68.4)	7(58.3)	5(23.8)		16(66.7)	4(50)	5(25)		12(70.6)	7(58.3)	6(26.1)		13(68.4)	7(58.3)	5(23.8)	
Triple-Negative	6(28.6)	1(10)	8(38.1)		5(26.3)	1(8.3)	9(42.9)		6(25)	0(0)	9(45)		4(23.5)	1(8.3)	10(43.5)		5(26.3)	1(8.3)	9(42.9)	
Hormonal receptors status				0.178				0.075				0.112				0.071				0.075
Negative	7(33.3)	5(50)	13(61.9)		6(31.6)	5(41.7)	14(66.7)		8(33.3)	4(50)	13(65)		5(29.4)	5(41.7)	15(65.2)		6(31.6)	5(41.7)	14(66.7)	
Positive	14(66.7)	5(50)	7(38.1)		13(68.4)	7(58.3)	7(33.3)		16(66.7)	4(50)	7(35)		12(70.6)	7(58.3)	8(34.8)		13(68.4)	7(58.3)	7(33.3)	
Her-2 status				**0.028**				0.061				**0.031**				0.115				0.061
Non-over-expressed	20(95.2)	6(60)	13(66.7)		18(94.7)	8(66.7)	14(66.7)		22(91.7)	4(50)	14(70)		16(94.1)	8(66.7)	16(69.6)		18(94.7)	6(66.7)	14(66.7)	
Over-expressed	1(4.8)	5(40)	6(33.3)		1(5.3)	4(33.3)	7(33.3)		2(8.3)	4(50)	6(30)		1(5.9)	4(33.3)	7(30.4)		1(5.3)	4(33.3)	7(33.3)	
Triple-Negative status				0.272				0.104				0.051				0.087				0.104
No	15(71.4)	9(90)	13(61.9)		14(73.7)	11(91.7)	12(57.1)		18(75)	8(1 0 0)	11(55)		13(76.5)	11(91.7)	13(56.5)		14(73.7)	11(91.7)	12(57.1)	
Yes	6(28.6)	1(10)	8(38.1)		5(26.3)	1(8.3)	9(42.9)		6(25)	0(0)	9(45)		4(23.5)	1(8.3)	10(43.5)		5(26.3)	1(8.3)	9(42.9)	
Luminal				**0.047**				**0.014**				**0.018**				**0.015**				**0.014**
No	7(33.3)	5(50)	15(71.4)		6(31.6)	5(41.7)	16(76.2)		8(33.3)	4(50)	15(75)		5(29.4)	5(41.7)	17(73.9)		6(31.6)	5(41.7)	16(76.2)	
Yes	14(66.7)	5(50)	6(28.6)		13(68.4)	7(58.3)	5(23.8)		16(66.7)	4(50)	5(25)		12(70.6)	7(58.3)	6(26.1)		13(68.4)	7(58.3)	5(28.8)	
Adjuvant Chemotherapy				0.52				0.423				0.459				0.459				0.423
No	7(33.3)	3(30)	4(19)		7(36.8)	2(16.7)	4(19)		6(25)	2(25)	5(25)		6(35.3)	3(25)	4(17.4)		7(36.8)	2(16.7)	4(19)	
Yes	14(85.7)	7(70)	17(81)		12(63.2)	10(83.3)	17(81)		18(75)	6(75)	1575)		11(64.7)	9(75)	19(82.6)		12(63.2)	10(83.3)	17(81)	
Adjuvant Radiotherapy				0.561				0.803				0.69				1				0.803
No	3(14.3)	3(30)	3(14.3)		3(15.8)	3(25)	3(14.3)		3(12.5)	2(25)	4(20)		3(17.6)	2(16.7)	4(17.4)		3(15.8)	3(25)	3(14.3)	
Yes	18(85.7)	7(70)	18(85.7)		16(84.2)	9(75)	18(85.7)		21(87.5)	6(75)	16(80)		14(82.4)	10(83.3)	19(82.6)		16(84.2)	9(75)	18(85.7)	

C1: cluster 1; C2: cluster 2; C3: cluster 3; [a]: mean (sd) or median (min, max).

Table 3
Comparison of prediction for overall and specific survival between clusters at 5 and 10-year.

		Predict 5-year				Predict 10-year			
		Overall Survival		Specific Survival		Overall Survival		Specific Survival	
Methods	No. of patients	% [95% CI]	P-value	% [95% CI]	P-value	% [95% CI]	P-value	% [95% CI]	P-value
K-sparse			**0.021**		**0.002**		**0.077**		**0.004**
	Cluster 1 (n = 19)	77% [67–82]		87% [80–91]		58% [48–65]		80% [73–86]	
	Cluster 2 (n = 12)	71% [57–82]		81% [69–90]		53% [38–66]		75% [60–85]	
	Cluster 3 (n = 20)	59% [47–69]		68% [60–74]		41% [29–52]		62% [53–69]	
SIMLR			0.1		**0.011**		0.241		**0.009**
	Cluster 1 (n = 17)	75% [64–82]		85% [77–91]		55% [45–64]		77% [65–84]	
	Cluster 2 (n = 12)	72% [56–82]		83% [69–90]		55% [40–67]		79% [65–87]	
	Cluster 3 (n = 22)	61% [50–70]		71% [63–77]		43% [32–53]		64% [55–70]	
Sparse K-means			**0.049**		**0.027**		0.203		**0.024**
	Cluster 1 (n = 24)	74% [64–80]		84% [76–89]		54% [43–63]		80% [73–86]	
	Cluster 2 (n = 7)	72% [58–87]		83% [70–94]		56% [37–72]		75% [60–85]	
	Cluster 3 (n = 20)	61% [49–69]		70% [61–78]		42% [32–52]		62% [53–69]	
Spectral clustering			**0.021**		**0.002**		0.077		**0.004**
	Cluster 1 (n = 19)	77% [68–83]		77% [80–91]		58% [48–65]		82% [73–86]	
	Cluster 2 (n = 12)	71% [57–81]		71% [69–90]		52% [32–64]		75% [60–85]	
	Cluster 3 (n = 20)	59% [47–68]		69% [60–76]		41% [29–52]		62% [53–69]	
PCA K-means			0.055		**0.009**		0.085		**0.008**
	Cluster 1 (n = 21)	77% [67–81]		86% [79–91]		58% [48–65]		79% [71–85]	
	Cluster 2 (n = 10)	69% [53–81]		80% [66–90]		52% [32–64]		77% [63–86]	
	Cluster 3 (n = 20)	60% [47–69]		69% [61–78]		41% [29–52]		63% [54–70]	

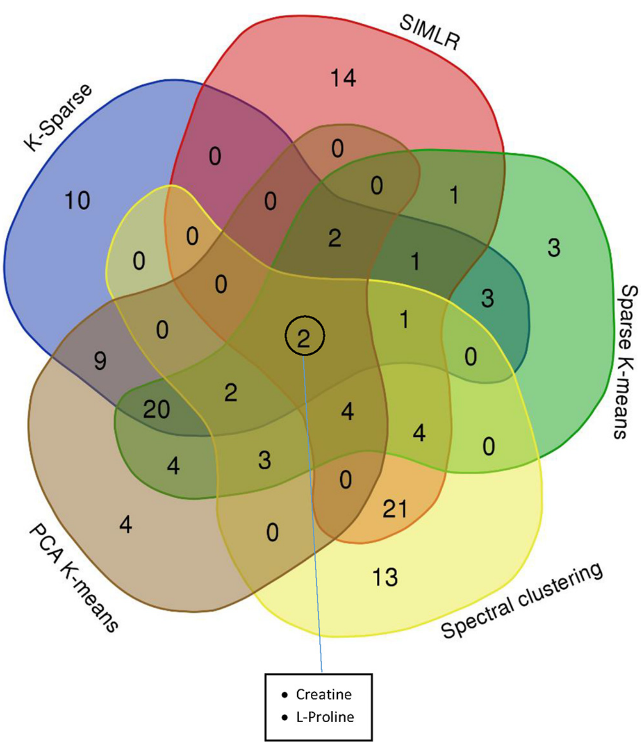

Fig. 3. Venn diagram of metabolic that were in common or unique to the five clustering methods.

means identified 10 pathways the 3 most important of which are "Alanine, aspartate and glutamate metabolism" involved in amino acid metabolic pathway, "Pyruvate metabolism" involved in carbohydrates metabolic/glucose oxidation pathway and "Citrate cycle (TCA cycle)" involved in energy metabolic pathway.

Finally, with 30 identified pathways, SIMLR is the method that identified the most metabolic pathways. Of these, the 3 most important highlighted metabolic pathways are "arginine and proline metabolism", "glycine, serine and threonine metabolism" and "alanine, aspartate and glutamate metabolism", involved in amino acid metabolic pathways. The Venn diagram (Fig. 4) shows the overlap of pathways detected by the five methods. Amino acid metabolism appeared to be the most frequently modified pathway. Enrichment and pathway analyses also showed modifications in glucose metabolism. From the biological point of view, SIMLR and spectral clustering are the two methods that identified the most relevant metabolic pathways.

3.2.7. Comparison of intensity of metabolites between the 5 methods

Among amino acid and glucose metabolisms, fourteen related metabolites were selected as potential biomarkers in BC [54–57]. As shown in Supplementary Fig. 4, the intensities of these 14 metabolites were compared between the 3 clusters for each of the 5 methods. The intensity of Uridine diphosphate (UDP) glucose, Guanine, L-Glutamine, L-Glutamic acid, L-Isoleucine, L-Proline, L-Methionine, L-Phenylalanine, Pyruvic acid, Spermine, Glutathione, Creatine, L-Carnitine and L-Acetylcarnitine were statistically significant between at least one of the clusters. The five methods agree that cluster 3 patients have low levels of Creatine, L-acetylcarnitine, L-Glutamic acid and high levels of Guanine, L-Isoleucine, L-Phenylalanine, Pyruvic acid and Spermine (Fig. 5). These metabolite levels seem to be predictive of poor prognosis [57–59].

4. Discussion

4.1. From a machine learning perspective

To the best of our knowledge, this proof-of-concept study is the first to compare different unsupervised ML methods to identify metabolomics-based prognostic signatures in BC. Analyses were performed intentionally without any prior clinical or biological assumptions. Clinical and biological interpretations were performed only after cluster identification. The objective of our study was to compare different unsupervised ML algorithms for feature selection from untargeted metabolomic data and to evaluate the capacity of these methods to select relevant features for further use in prediction models. This study did not seek to highlight significant differences but rather to assess how unsupervised methods might behave with high-dimension metabolic data and to open up new perspectives in the particularly active domain of BC

Table 4
Table indicating which metabolites are in each intersection or are unique to a certain list.

	Clustering Methods	Nbr	Metabolites
5	K-Sparse PCA K-means SIMLR Sparse K-means Spectral clustering	2	Creatine; L-Proline;
4	K-Sparse SIMLR Sparse K-means Spectral clustering	1	Triethanolamine;
	K-Sparse PCA K-means SIMLR Sparse K-means	2	L-Methionine; L-Phenylalanine
	K-Sparse PCA K-means Sparse K-means Spectral clustering	2	L-Carnitine; Betaine;
	PCA K-means SIMLR Sparse K-means Spectral clustering	4	Glutathione; Isoleucyl-Methionine; Humulinic acid A; Alnustone;
3	K-Sparse SIMLR Sparse K-means	1	Hydroxyprolyl-Valine;
	K-Sparse PCA K-means Sparse K-means	20	Aminoadipic acid; Methylmalonic acid; 1b-Furanoeudesm-4(15)-en-1-ol acetate; Glycerophosphocholine; Lidocaine; Adenosine monophosphate; 2-Methyl-3-ketovaleric acid; Liqcoumarin; p-Cresol sulfate; 2-Methylbutyroylcarnitine; Methoxsalen; Citramalic acid; Hypoxanthine; L-Acetylcarnitine; Ethyl aconitate; Guanine; L-Glutamic acid; Uridine 5′-monophosphate; N1,N12-Diacetylspermine; 5-Aminoimidazole ribonucleotide
	SIMLR Sparse K-means Spectral clustering	4	2,5-Dichloro-4-oxohex-2-enedioate; Histidinyl-Isoleucine; 3-(4-Methyl-3-pentenyl)thiophene; (−)-Epigallocatechin
	PCA K-means Sparse K-means Spectral clustering	3	L-Isoleucine; Ascorbic acid; Neurine;
2	K-Sparse Sparse K-means	3	5-Hydroxyisourate; Hexanoylcarnitine; L-Glutamine;
	K-Sparse PCA K-means	9	Creatinine; Proline; betaine; Erythronic acid; Garcinia acid; Thiolutin; 4-Chloro-1H-indole-3-acetic acid; Niacinamide 3-Dehydroxycarnitine; Dihydrothymine;
	SIMLR Spectral clustering	21	5b-Cyprinol sulfate; 2′,4-Dihydroxy-4′,6′-dimethoxychalcone; Propenoylcarnitine; 5-Hydroxyindoleacetic acid; Phaseolic acid Lisuride; 2-Bromophenol; (alpha-D-mannosyl)7-beta-D-mannosyl-diacetylchitobiosyl-L-asparagine isoform B (protein); Plastoquinone 3; 2,2,4,4,-Tetramethyl-6-(1-oxopropyl)-1,3,5-cyclohexanetrione; 1-Pyrroline; Gingerol; Prehumulinic acid; 1-Methylpyrrolo[1,2-a]pyrazine; 5-(methylthio)-2,3-Dioxopentyl phosphate; Propionic acid; Isosakuranin; Phenmetrazine; Methionine sulfoxide; Glycerol; Carboxyphosphamide
	SIMLR Sparse K-means	1	Phosphoric acid;
	PCA K-means Sparse K-means	4	I(−); L-Tyrosine; Gravelliferone; Valganciclovir;
1	K-Sparse	10	Prolylhydroxyproline; Guanidoacetic acid; Histamine; PC-M6; L-Histidine; N-Acetyl-L-aspartic acid; 3-Mercaptohexyl hexanoate; Trimethylamine N-oxide; Pantothenic acid; Flunitrazepam
	SIMLR	14	3-Hydroxy-6,8-dimethoxy-7(11)-eremophilen-12,8-olide; Glycerol tripropanoate; Alanyl-Isoleucine; 1-(2,4,6-Trimethoxyphenyl)-1,3-butanedione; 1-Oxo-1H-2-benzopyran-3-carboxaldehyde; 1,3,11-Tridecatriene-5,7,9-triyne; N-Acetyl-L-methionine; 3-Methyl sulfolene; 5-(4-Acetoxy-3-oxo-1-butynyl)-2,2′-bithiophene; Ac-Ser-Asp-Lys-Pro-OH; Cyclic AMP; Benzothiazole; (±)-2-Methylthiazolidine; 2-Methylcitric acid
	Spectral clustering	13	2,3-diketogulonate; 2,5-Furandicarboxylic acid; Pyrrolidine; Piperidine; Beta-Alanine; Aspartyl-L-proline; Erythro-5-hydroxy-L-lysinium(1 +); Acrylamide; 5-Hydroxylysine; S-Nitrosoglutathione; 2,2-dichloro-1,1-ethanediol; Valerenic acid; Dichloromethane
	Sparse K-means	3	Erinapyrone C; Ergothioneine; N-Methylethanolaminium phosphate
	PCA K-means	4	Dimethylglycine; Pipecolic acid; Methyl (9Z)-10′-oxo-6,10′-diapo-6-carotenoate; N-Desmethylvenlafaxine

phenotype predictors. We demonstrated that the K-sparse and SIMLR methods have a higher clustering performance compared with the three other popular unsupervised ML methods in detecting groups of patients with BC using metabolomic data. Interestingly, even though the spectral method is a little less clinically efficient than the k-sparse and SIMLR methods, it identified relevant metabolic pathways.

Our study suffers from various limitations, namely the relatively small number of patients and the monocentric and retrospective nature of the study. Besides, our results could not be validated on an external cohort. The clustering performances were assessed only by internal validation based on silhouette value. Indeed, we could not compare the labels obtained from our classification with the true labels to calculate the accuracy of the classification since the true labels were unknown.

Other unsupervised ML methods such as model-based clustering, bi-clustering and deep learning may be of value in this analysis and should be further explored. Yet it is worth noting that, even

Table 5
List of significant relevant pathways identified by 5 methods.

K-Sparse method

Clusters Comparaison	Interaction metabolite	Pathway Name	Total Cmpd[a]	Match Status[b]	Raw P[c]	-log(p)	Impact[d]
C1 vs C3	UDP – glucose	Starch and sucrose metabolism	50	1	0,0107	4,5388	0,1390
	UDP – glucose	Amino sugar and nucleotide sugar metabolism	88	1	0,0107	4,5388	0,0928
	UDP - glucose; Glyceric acid	Glycerolipid metabolism	32	2	0,0153	4,1831	0,0206

SIMLR method

Clusters Comparaison	Interaction metabolite	Pathway Name	Total Cmpd	Match Status	P Value	-log(p)	Impact
C1 VS C2	Glutathione; Oxidized glutathione; Glycine; L-Glutamic acid; Pyroglutamic acid; Spermidine; Ornithine; Putrescine; Spermine; Cadaverine; Aminopropylcadaverine; Ascorbic acid	Glutathione metabolism	38	12	0	12,826	0,3628
	Ascorbic acid; Uridine diphosphate glucose; Pyruvic acid; D-Glucuronic acid 1-phosphate; Oxoglutaric acid;	Ascorbate and aldarate metabolism	45	5	0	12,469	0,1383
	L-Tryptophan; N-Acetylserotonin; 5-Hydroxyindoleacetic acid; 2-Aminomuconic acid semialdehyde; 3-Hydroxyanthranilic acid; L-Kynurenine; Acetyl-N-formyl-5-methoxykynurenamine; Isophenoxazine;	Tryptophan metabolism	79	8	0,0001	9,1233	0,2741
	5′-Methylthioadenosine; N-Formyl-L-methionine; L-Homocysteine; L-Methionine; Glutathione; Phosphoserine; 3-Sulfinoalanine; L-Aspartyl-4-phosphate; Pyruvic acid;	Cysteine and methionine metabolism	56	9	0,0008	7,1674	0,2509
	L-Glutamine; Phosphoribosylformylglycineamidine; Cyclic AMP; Adenosine monophosphate; Adenosine; Inosine; Adenine; Hypoxanthine; Guanine; Uric acid; 5-Hydroxyisourate; Guanosine; Adenosine diphosphate ribose; 5-Aminoimidazole ribonucleotide; Glyoxylic acid; Glycine; Adenosine 3′,5′-diphosphate;	Purine metabolism	92	17	0,0011	6,8091	0,2048
	Glyoxylic acid; Oxoglutaric acid; N-Formyl-L-methionine; Glycolic acid; Glyceric acid; Pyruvic acid;	Glyoxylate and dicarboxylate metabolism	50	6	0,0027	5,9281	0,268
	L-Glutamine; Ornithine; Citrulline; L-Arginine; L-Glutamic acid; N-Acetylornithine; L-Proline; Hydroxyproline; Guanidoacetic acid; Creatine; 4-Guanidinobutanoic acid; N2-Succinyl-L-ornithine; Putrescine; Spermidine; N-Acetylputrescine; Pyruvic acid; Glyoxylic acid; Spermine;	Arginine and proline metabolism	77	19	0,0053	5,238	0,6514
	Oxoglutaric acid; Oxalosuccinic acid; Pyruvic acid;	Citrate cycle (TCA cycle)	20	3	0,0075	4,8991	0,176
	D-Xylose; Uridine diphosphate glucose; D-Glucuronic acid 1-phosphate; Pyruvic acid;	Pentose and glucuronate interconversions	53	4	0,0076	4,8821	0,0394
	2-Hydroxyethanesulfonate; Pyruvic acid; 3-Sulfinoalanine;	Taurine and hypotaurine metabolism	20	3	0,0154	4,1754	0,0324
	Glyceric acid; Betaine; Guanidoacetic acid; Dimethylglycine; Glycine; Phosphoserine; L-Threonine; O-Phosphohomoserine; L-Aspartyl-4-phosphate; Creatine; Glyoxylic acid; Pyruvic acid; L-Tryptophan	Glycine, serine and threonine metabolism	48	13	0,018	4,0154	0,46986
	Uridine diphosphate glucose; D-Glucuronic acid 1-phosphate; N-Acetyl-D-Glucosamine 6-Phosphate; Uridine diphosphate-N-acetylglucosamine; Cytidine monophosphate N-acetylneuraminic acid; D-Glucose; D-Xylose	Amino sugar and nucleotide sugar metabolism	88	7	0,0187	3,9783	0,1417
	Formiminoglutamic acid; L-Glutamic acid; Urocanic acid; L-Histidine; Histamine; D-Erythro-imidazole-glycerol-phosphate; Ergothioneine; Hydantoin-5-propionic acid; Imidazole acetol-phosphate; Oxoglutaric acid;	Histidine metabolism	44	10	0,0412	3,1903	0,3705
	Pyridoxamine; Oxoglutaric acid; 3-Hydroxy-2-methylpyridine-4,5-dicarboxylate; Pyruvic acid;	Vitamin B6 metabolism	32	4	0,0412	3,1898	0,0773
C1 VS C3	Formiminoglutamic acid; L-Glutamic acid; Urocanic acid; L-Histidine; Histamine; D-Erythro-imidazole-glycerol-phosphate; Ergothioneine; Hydantoin-5-propionic acid; Imidazole acetol-phosphate; Oxoglutaric acid;	Histidine metabolism	44	10	0,0139	4,2752	0,3705
	Phenylpyruvic acid; L-Phenylalanine; L-Tyrosine; 3-Dehydroquinate; L-Tryptophan;	Phenylalanine, tyrosine and tryptophan biosynthesis	27	5	0,0189	3,9687	0,099
	L-Tryptophan; N-Acetylserotonin; 5-Hydroxyindoleacetic acid; 2-Aminomuconic acid semialdehyde; 3-Hydroxyanthranilic acid; L-Kynurenine; Acetyl-N-formyl-5-methoxykynurenamine; Isophenoxazine;	Tryptophan metabolism	79	8	0	16,409	0,2741
C2 VS C3	Glutathione; Oxidized glutathione; Glycine; L-Glutamic acid; Pyroglutamic acid; Spermidine; Ornithine; Putrescine; Spermine; Cadaverine; Aminopropylcadaverine; Ascorbic acid;	Glutathione metabolism	38	12	0	16,133	0,3628
	Ascorbic acid; Uridine diphosphate glucose; Pyruvic acid; D-Glucuronic acid 1-phosphate; Oxoglutaric acid	Ascorbate and aldarate metabolism	45	5	0	13,096	0,1383
	5′-Methylthioadenosine; N-Formyl-L-methionine; L-Homocysteine; L-Methionine; Glutathione; Phosphoserine; 3-Sulfinoalanine; L-Aspartyl-4-	Cysteine and methionine	56	9	0,0001	9,8548	0,2509

(continued on next page)

Table 5 (*continued*)

SIMLR method

Clusters Comparaison	Interaction metabolite	Pathway Name	Total Cmpd	Match Status	P Value	-log(p)	Impact
	phosphate; Pyruvic acid;	metabolism					
	Phenylpyruvic acid; L-Phenylalanine; L-Tyrosine; 3-Dehydroquinate; L-Tryptophan;	Phenylalanine, tyrosine and tryptophan biosynthesis	27	5	0,0001	8,9814	0,099
	L-Histidine; L-Phenylalanine; L-Arginine; L-Glutamine; Glycine; L-Methionine; L-Lysine; L-Isoleucine; L-Threonine; L-Tryptophan; L-Tyrosine; L-Proline; L-Glutamic acid; Phosphoserine;	Aminoacyl-tRNA biosynthesis	75	14	0,0002	8,758	0,1127
	Glyoxylic acid; Oxoglutaric acid; N-Formyl-L-methionine; Glycolic acid; Glyceric acid; Pyruvic acid;	Glyoxylate and dicarboxylate metabolism	50	6	0,0004	7,7271	0,268
	L-Glutamine; Phosphoribosylformylglycineamidine; Cyclic AMP; Adenosine monophosphate; Adenosine; Inosine; Adenine; Hypoxanthine; Guanine; Uric acid; 5-Hydroxyisourate; Guanosine; Adenosine diphosphate ribose; 5-Aminoimidazole ribonucleotide; Glyoxylic acid; Glycine; Adenosine 3′,5′-diphosphate;	Purine metabolism	92	17	0,0007	7,306	0,2048
	Malonic acid; Beta-Alanine; Spermine; Spermidine; Dihydrouracil; Pantothenic acid; Uracil; L-Histidine	beta-Alanine metabolism	28	8	0,0012	6,7568	0,3577
	Uridine 5′-monophosphate; L-Glutamine; Dihydrouracil; Cytidine monophosphate; Cytidine; Cytosine; Uracil; Dihydrothymine; Uridine diphosphate glucose; Malonic acid; Ureidosuccinic acid; Beta-Alanine; Methylmalonic acid;	Pyrimidine metabolism	60	13	0,0014	6,5817	0,2756
	Pantothenic acid; Dihydrouracil; Beta-Alanine; Pyruvic acid; Adenosine 3′,5′-diphosphate; Uracil;	Pantothenate and CoA biosynthesis	27	6	0,0023	6,0879	0,2736
	L-Phenylalanine; Phenylpyruvic acid; Benzoic acid; Hippuric acid; Pyruvic acid; L-Tyrosine;	Phenylalanine metabolism	45	6	0,0072	4,9364	0,2468
	L-Glutamic acid; L-Glutamine; Oxoglutaric acid	D-Glutamine and D-glutamate metabolism	11	3	0,0124	4,39	0,139
	L-Glutamine; Ornithine; Citrulline; L-Arginine; L-Glutamic acid; N-Acetylornithine; L-Proline; Hydroxyproline; Guanidoacetic acid; Creatine; Creatinine; 4-Guanidinobutanoic acid; N2-Succinyl-L-ornithine; Putrescine; Spermidine; N-Acetylputrescine; Pyruvic acid; Glyoxylic acid; Spermine;	Arginine and proline metabolism	77	19	0,0169	4,082	0,6514
	2-Hydroxyethanesulfonate; Pyruvic acid; 3-Sulfinoalanine;	Taurine and hypotaurine metabolism	20	3	0,0215	3,8411	0,0324
	N-Acetyl-L-aspartic acid; Pyruvic acid; Ureidosuccinic acid; Oxoglutaric acid; L-Glutamine; L-Glutamic acid; 2-Keto-glutaramic acid;	Alanine, aspartate and glutamate metabolism	24	7	0,0221	3,8108	0,4122
	Pyridoxamine; Oxoglutaric acid; 3-Hydroxy-2-methylpyridine-4,5-dicarboxylate; Pyruvic acid;	Vitamin B6 metabolism	32	4	0,0267	3,6235	0,0773
	Oxoglutaric acid; Oxalosuccinic acid; Pyruvic acid	Citrate cycle (TCA cycle)	20	3	0,0302	3,5015	0,176
	Glyceric acid; Betaine; Guanidoacetic acid; Dimethylglycine; Glycine; Phosphoserine; L-Threonine; O-Phosphohomoserine; L-Aspartyl-4-phosphate; Creatine; Glyoxylic acid; L-Tryptophan	Glycine, serine and threonine metabolism	48	13	0,0372	3,2914	0,4699
	Uridine diphosphate glucose; Glycerol 3-phosphate; Glycerol; Glyceric acid; Galactosylglycerol;	Glycerolipid metabolism	32	5	0,0427	3,1546	0,2162
	D-Xylose; Uridine diphosphate glucose; D-Glucuronic acid 1-phosphate; Pyruvic acid;	Pentose and glucuronate interconversions	53	4	0,0427	3,1536	0,0394

Sparse K-means method

Clusters Comparaison	Interaction metabolite		Total Cmpd	Match Status	Raw p	-log(p)	Impact
C1 VS C2	L-Methionine; Glutathione	Cysteine and methionine metabolism	56	2	0.007	4.9	0.0454
C1 VS C3	L-Methionine; Glutathione;	Cysteine and methionine metabolism	56	2	0.0020	6.2	0.00454

Spectral clustering method

Clusters Comparaison	Interaction metabolite	Pathway Name	Total Cmpd	Match Status	Raw p	-log(p)	Impact
C1 VS C3	Iminoaspartic acid; Quinolinic acid; Niacinamide; Pyruvic acid; Propionic acid;	Nicotinate and nicotinamide metabolism	44	5	0,0024	6,0206	0,0712
	Glyceric acid; Betaine; Guanidoacetic acid; Dimethylglycine; Glycine; Phosphoserine; L-Threonine; O-Phosphohomoserine; L-Aspartyl-4-phosphate; Creatine; Glyoxylic acid; L-Tryptophan	Glycine, serine and threonine metabolism	48	13	0,0040	5,5100	0,4699

Table 5 (*continued*)

Spectral clustering method

Clusters Comparaison	Interaction metabolite	Pathway Name	Total Cmpd	Match Status	Raw p	-log(p)	Impact
	5′-Methylthioadenosine; N-Formyl-L-methionine; L-Homocysteine; L-Methionine; Glutathione; Phosphoserine; 3-Sulfinoalanine; L-Aspartyl-4-phosphate; Pyruvic acid;	Cysteine and methionine metabolism	56	9	0,0098	4,6232	0,2509
	Formiminoglutamic acid; L-Glutamic acid; Urocanic acid; L-Histidine; Histamine; D-Erythro-imidazole-glycerol-phosphate; Ergothioneine; Hydantoin-5-propionic acid; Imidazole acetol-phosphate; Oxoglutaric acid;	Histidine metabolism	44	10	0,0101	4,5961	0,3705
	xoglutaric acid; Oxalosuccinic acid; Pyruvic acid;	Citrate cycle (TCA cycle)	20	3	0,0171	4,0710	0,1760
	Pyruvic acid; L-Threonine; L-Isoleucine;	Valine, leucine and isoleucine biosynthesis	27	3	0,0178	4,0277	0,0350
	D-Xylose; Uridine diphosphate glucose; D-Glucuronic acid 1-phosphate; Pyruvic acid;	Pentose and glucuronate interconversions	53	4	0,0210	3,8609	0,0394
	D-Glucose; Glyceric acid; Pyruvic acid;	Pentose phosphate pathway	32	3	0,0232	3,7622	0,0218
	Pyruvic acid; L-Lactic acid; D-Glucose;	Glycolysis or Gluconeogenesis	31	3	0,0249	3,6928	0,0953
	Pyruvic acid; L-Lactic acid;	Pyruvate metabolism	32	2	0,0274	3,5955	0,3201
	L-Glutamic acid; Pyruvic acid; Butyric acid; Oxoglutaric acid;	Butanoate metabolism	40	4	0,0283	3,5644	0,0852
	2-Hydroxyethanesulfonate; Pyruvic acid; 3-Sulfinoalanine;	Taurine and hypotaurine metabolism	20	3	0,0287	3,5525	0,0324
	Glyoxylic acid; Oxoglutaric acid; N-Formyl-L-methionine; Glycolic acid; Glyceric acid; Pyruvic acid;	Glyoxylate and dicarboxylate metabolism	50	6	0,0303	3,4966	0,2680
	Ascorbic acid; Uridine diphosphate glucose; Pyruvic acid; D-Glucuronic acid 1-phosphate; Oxoglutaric acid;	Ascorbate and aldarate metabolism	45	5	0,0330	3,4104	0,1383
	Epinephrine; Dopamine; L-Tyrosine; Homovanillic acid; Pyruvic acid;	Tyrosine metabolism	76	5	0,0385	3,2580	0,1750
	N-Acetyl-L-aspartic acid; Pyruvic acid; Ureidosuccinic acid; Oxoglutaric acid; L-Glutamine; L-Glutamic acid; 2-Keto-glutaramic acid;	Alanine, aspartate and glutamate metabolism	24	7	0,0390	3,2431	0,4122
	Pyridoxamine; Oxoglutaric acid; 3-Hydroxy-2-methylpyridine-4,5-dicarboxylate; Pyruvic acid;	Vitamin B6 metabolism	32	4	0,0447	3,1074	0,0773

PCA K-means method

Clusters Comparaison	Interaction metabolite	Pathway Name	Total Cmpd	Match Status	Raw p	-log(p)	Impact
C1 vs C3	Iminoaspartic acid; Quinolinic acid; Niacinamide; Pyruvic acid; Propionic acid;	Nicotinate and nicotinamide metabolism	44	5	0,003	5,9412	0,0712
	Oxoglutaric acid; Oxalosuccinic acid; Pyruvic acid;	Citrate cycle (TCA cycle)	20	3	0,011	4,4865	0,1760
	Epinephrine; Dopamine; L-Tyrosine; Homovanillic acid; Pyruvic acid;	Tyrosine metabolism	76	5	0,024	3,7311	0,1750
	Pyruvic acid; L-Lactic acid;	Pyruvate metabolism	32	2	0,043	3,1507	0,3201
	D-Xylose; Uridine diphosphate glucose; D-Glucuronic acid 1-phosphate; Pyruvic acid;	Pentose and glucuronate interconversions	53	4	0,044	3,1214	0,0394
	Pyruvic acid; L-Threonine; L-Isoleucine;	Valine, leucine and isoleucine biosynthesis	27	3	0,045	3,1107	0,0350
	Ascorbic acid; Uridine diphosphate glucose; Pyruvic acid; D-Glucuronic acid 1-phosphate; Oxoglutaric acid;	Ascorbate and aldarate metabolism	45	5	0,045	3,0926	0,1383
	L-Glutamic acid; Pyruvic acid; Butyric acid; Oxoglutaric acid;	Butanoate metabolism	40	4	0,046	3,0843	0,0852
	D-Glucose; Glyceric acid; Pyruvic acid;	Pentose phosphate pathway	32	3	0,046	3,0769	0,0218
	N-Acetyl-L-aspartic acid; Pyruvic acid; Ureidosuccinic acid; Oxoglutaric acid; L-Glutamine; L-Glutamic acid; 2-Keto-glutaramic acid	Alanine, aspartate and glutamate metabolism	24	7	0,048	3,0446	0,4122

[a] Total cmpd is the total number of compounds in the pathway.
[b] Hits is the actual matched number from the uploaded data.
[c] Raw p is the original *p*-value calculated from the pathway analysis.
[d] Impact is the pathway impact value calculated from pathway topology analysis.

though deep learning methods are of particular interest in many fields, they necessitate a very large number of patients to be efficiently trained and may therefore not be suitable for small metabolomics datasets obtained on real life patients, such as the one we have used. While obtaining imaging or clinical data concerning several thousands of patients seems achievable, obtaining metabolomics data for that many patients is currently much more complicated. Furthermore, even though some efforts are being made to tackle this issue [60], it is currently impossible to understand which features are responsible for the outcome when using deep-learning clustering techniques. It would therefore be impossible to understand the metabolic differences underlying different patient clusters if deep learning clustering was used.

These considerations raise important questions: in the future, on what basis should decisions be made? On results from a single method? Or on results provided by several methods? In view of the

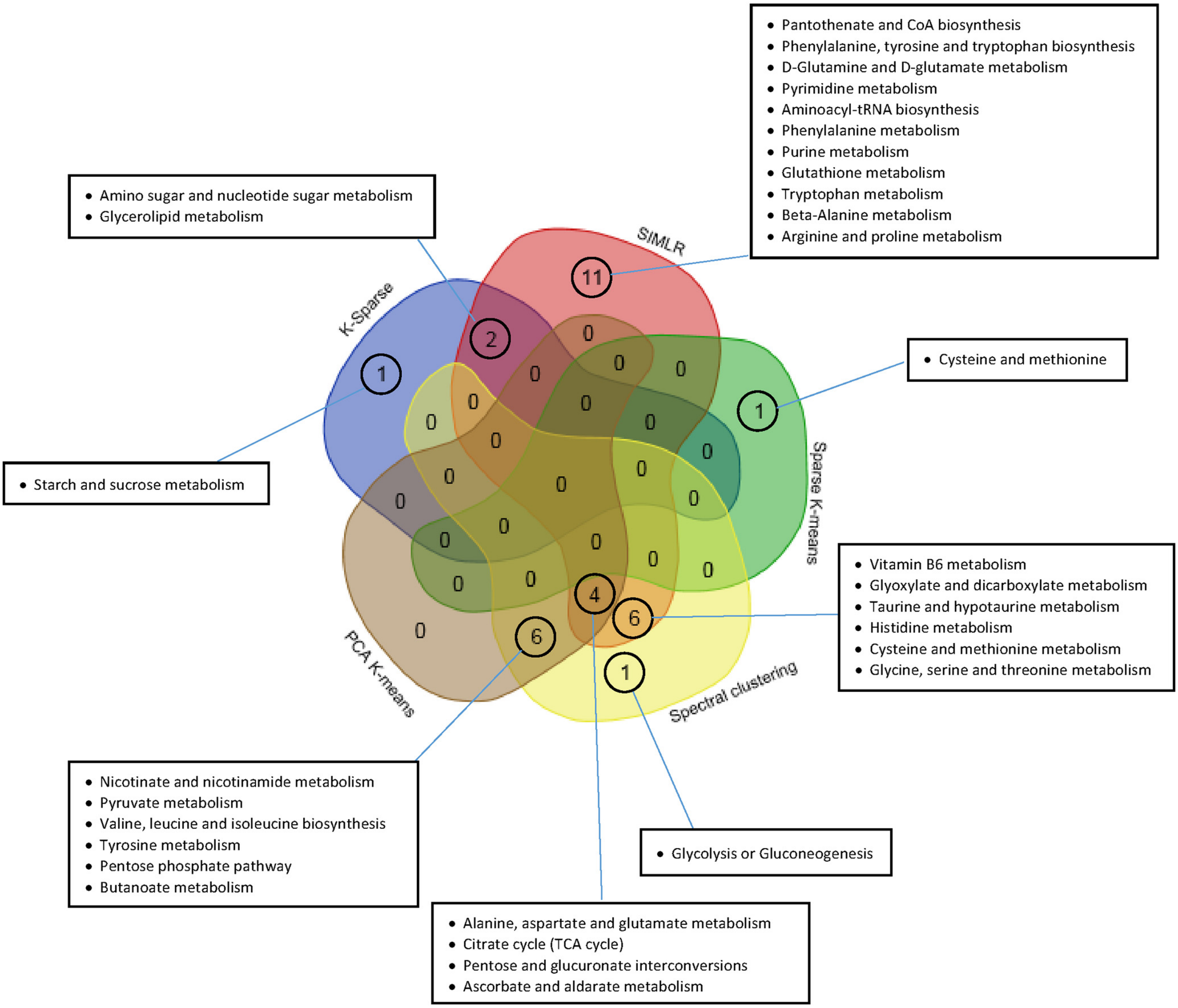

- Amino sugar and nucleotide sugar metabolism
- Glycerolipid metabolism

- Pantothenate and CoA biosynthesis
- Phenylalanine, tyrosine and tryptophan biosynthesis
- D-Glutamine and D-glutamate metabolism
- Pyrimidine metabolism
- Aminoacyl-tRNA biosynthesis
- Phenylalanine metabolism
- Purine metabolism
- Glutathione metabolism
- Tryptophan metabolism
- Beta-Alanine metabolism
- Arginine and proline metabolism

- Cysteine and methionine

- Starch and sucrose metabolism

- Vitamin B6 metabolism
- Glyoxylate and dicarboxylate metabolism
- Taurine and hypotaurine metabolism
- Histidine metabolism
- Cysteine and methionine metabolism
- Glycine, serine and threonine metabolism

- Nicotinate and nicotinamide metabolism
- Pyruvate metabolism
- Valine, leucine and isoleucine biosynthesis
- Tyrosine metabolism
- Pentose phosphate pathway
- Butanoate metabolism

- Glycolysis or Gluconeogenesis

- Alanine, aspartate and glutamate metabolism
- Citrate cycle (TCA cycle)
- Pentose and glucuronate interconversions
- Ascorbate and aldarate metabolism

Fig. 4. Venn diagram of pathways that were in common or unique to the five clustering methods.

findings we have highlighted, it seems that decisions should be taken collegially, i.e. based on the results of a set of methods, as at multidisciplinary consultation meetings involving health professionals from different disciplines and whose skills are essential to take decisions ensuring patients the best possible care according to the state of the science.

4.2. From a clinical perspective

From a clinical point of view, the methods were able to highlight three distinct groups of patients with different clinical profiles. Patients identified in cluster 1 may be considered to have the best prognosis, patients in cluster 2 an intermediate prognosis, while patients in cluster 3 may be considered to have the worst prognosis. The results in Table 2 show that the tumors of patients in cluster 1 were predominantly non-invasive and non-proliferative, whereas the tumors of cluster 3 patients were mainly invasive and proliferative. Tumors in cluster 2 were rather invasive but not proliferative, hence the intermediate prognosis. We hypothesize that these patients would have an intermediate (atypical) biological profile, which is why the methods are discordant. We further evidence heterogeneity within the triple-negative BC subpopulation with most of the patients classified in cluster 3. However, a third of the triple-negative patients were in cluster 1 Recent molecular profiling studies of triple-negative BC using parallel sequencing and other "omics" technologies have also uncovered an unexpectedly high level of heterogeneity as well as a number of common features [61,62].

In addition, no significant difference between clusters could be demonstrated in terms of age, histologic type, lymph node involvement, metastasis or survival (OS, SS or RFS). Indeed, with a median follow-up of only 48.5 months, this duration is insufficient to demonstrate a significant difference in terms of OS, SS, or RFS. Nevertheless, it is quite easy to predict that patients in cluster 3 have the highest risk of progression and that, conversely, patients in cluster 1 have the lowest risk of progression. To confirm this intuition and try to reduce this short follow-up limitation, we analyzed simulated survival data obtained with the PREDICT tool. With a 5-year pOS rate at around 75% for cluster 1, 70% for cluster 2 and 60% for cluster 3, *in-silico* analyses have demonstrated their high potential value [28,63,64] and confirmed that patients in cluster 3 have a poorer prognosis [65,66]. One limitation of our study could be the

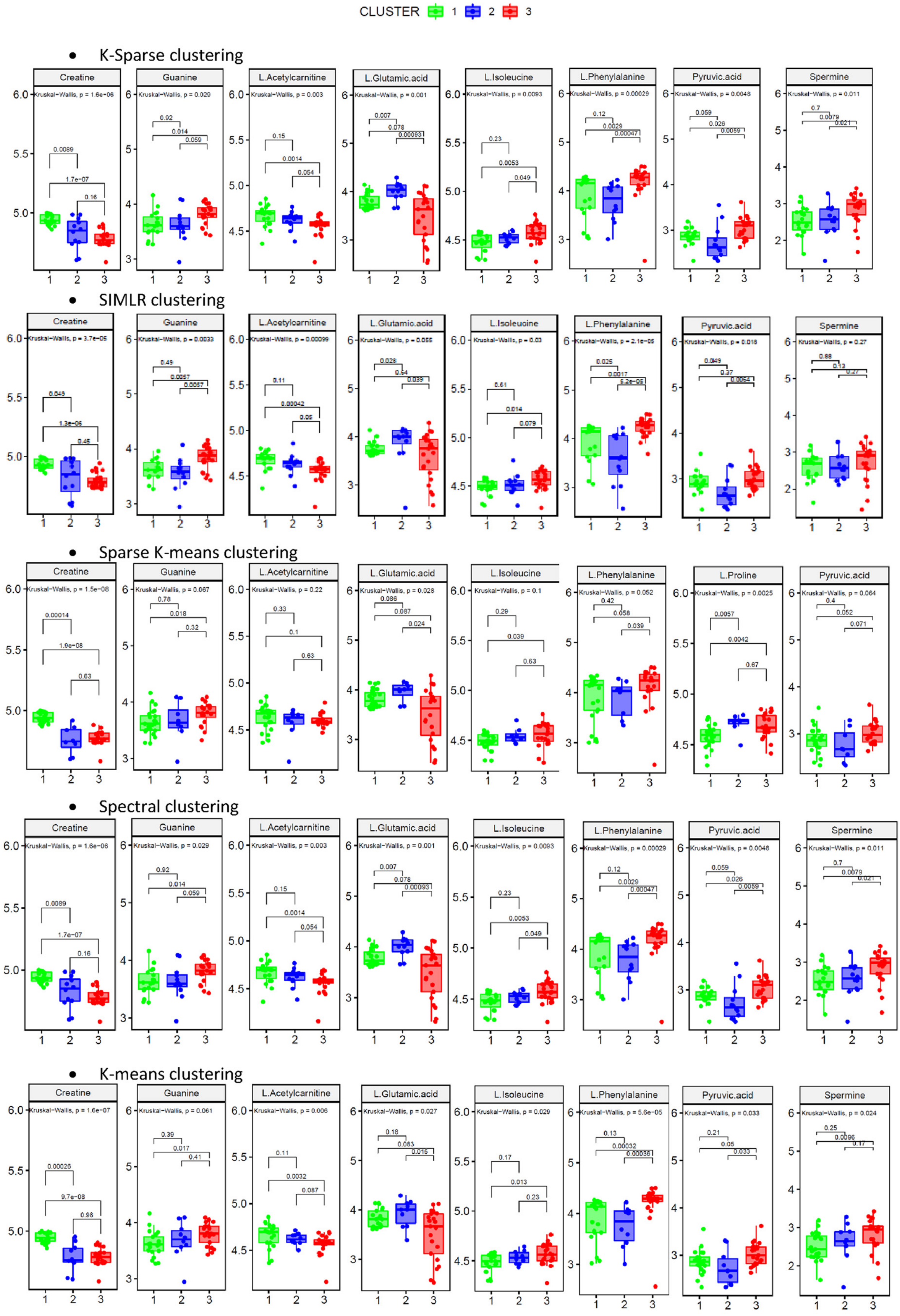

Fig. 5. Boxplot of the 8 metabolites extracted from 5 ML methods.

representativity of our population, e.g. it is recognized that BCs in younger patients (<40 years) are more aggressive [67]. Our study did not include a large number of young patients, which could explain why no significant difference was demonstrated in terms of age between clusters. Similarly, with only three patients with invasive lobular carcinoma (6%), our results did not identify a metabolic signature associated with this phenotype. Previous studies have shown a survival benefit in favor of invasive lobular carcinoma [68,69] and metabolomic studies focused on this particular type of BC could provide valuable biological information. Furthermore, due to the over-representation of hormonal-receptor negative tumors (48%) in our population compared to the literature [70], our population could have had unfavorable prognosis. This bias may result from our method of tumor selection. We decided to analyze frozen samples available in our biobank. Obviously, hormonal-receptor negative, triple-negative, Her-2-positive tumors are more often frozen and stored for further molecular testing and inclusion in clinical trials. In the present study, it is interesting to note that the five methods classified 73% of the patients in the same cluster. Among the 27% of patients classified differently by at least one of the methods, 9.5% of patients were classified heterogeneously by the five methods. Indeed, for each of these 5 patients, three methods classified them in one cluster and 2 others in another cluster without any connection between the types of methods used. Moreover, it is interesting to note that the different methods classified patients, on the one hand, in either the good prognostic cluster or the intermediate prognostic cluster or, on the other, in either the intermediate prognostic cluster or the poor prognostic cluster, but never in the good prognostic cluster or the poor prognostic cluster. A clinical analysis of these 5 patients showed that they had atypical clinical profiles, probably due to particular biological profiles. These atypical profiles would explain why no classification consensus could be highlighted. Overall, ML methods must remain a decision-making tool for the clinician, especially in cases where patients have particular clinical and biological characteristics. To avoid possible medical errors, the final responsibility for the decision lies with the clinician [71].

Finally, the initial clinical objective of this study was to define a metabolomic signature to refine the current classification and help the clinician in his chemotherapy prescription. This paper is the result of methodological research analyzing the best ML methods to develop this new tool. The patients selected were therefore patients eligible for adjuvant chemotherapy. An analysis of the metastatic population could help define a specific signature of metastatic status and/or a signature associated to survival. However, the use of biopsy faces two practical difficulties: 1) the intratumoral and inter-site heterogeneity that could be overcome through the analysis of blood or urine samples; and 2) the amount of material available once the pathologic analyses essential for patient management have been performed. Metabolomic analysis on paraffin slides could facilitate access to specimens and limit the amount of material required.

4.3. From a biological perspective

From a physiological point-of-view, this study extends the molecular stratification of BC to metabolomic profiles. Indeed, our results suggest that dysregulation of metabolic pathways exists between BC subtypes and that a particular amino acid profile characterizes the different BC histologic subtypes. Dysregulations of amino acid metabolism are well-known key events during cancer development [72] and are emerging hallmarks of cancers [73,74]. Amino acids serve not only as building blocks in protein synthesis but also as energy sources favoring cancer cell proliferation and growth [75]. Of interest, we identified significant differences between the BC subtypes of three metabolic pathways (i.e. Glycolysis and lactate production, Glutaminolysis, and amino acid) that play a pivotal role in BC growth [76,77]. Using the five methods, we consistently found that patients in cluster 3 showed higher levels of Guanine, L-Isoleucine, L Methionine, L-Phenylalanine, Pyruvic acid, Spermine and low levels of Creatine, L-Acetylcarnitine and L-Glutamic acid. Our results suggested that these metabolites could be candidate biomarker predictors of poorer prognosis [78–82]. All these results are consistent with the literature [57,83–86].

Given the exploratory nature of our study, we decided to use an FDR rate of 0.25 as a threshold in order to identify relevant candidate pathways (https://software.broadinstitute.org/cancer/software/gsea/wiki/index.php/FAQ).

A validation of these pathways, during a study whose main objective will be to evaluate the usefulness of our metabolomics signatures for decision-making, will need to be established with the use of a lower False Discovery Rate or Family Wise Error Rate (<0.05).

Indeed, to meet the biosynthetic needs associated with rapid proliferation, cancer cells must increase the import of nutrients. Two main metabolites are essential for biosynthesis and survival in mammalian cells, and particularly in cancer cells: glucose [87] and glutamine [88]. The increased glucose uptake in tumors compared to other healthy and non-proliferative tissues was first described more than 90 years ago by Otto Warburg [89]. Glucose is the primary energy source of all cells because of its involvement in many processes such as glycolysis or the Krebs cycle [90] in mitochondria. Unlike healthy cells that adapt to available substrates (glucose/fatty acids/proteins), some tumor cells are addicted to glucose. The other important point is that, once metabolized, tumor cells will prefer lactic fermentation to the Krebs cycle.

Lastly, the precise etiology of BC is still unknown even though some genetic, epigenetic and environmental factors have been identified [91]. It has been conclusively demonstrated that cancer cell metabolism is heavily influenced by microenvironmental factors, including nutrient availability. Sullivan and coworkers [92] found that diet affects local nutrient availability. This effect can lead to substantial changes in the metabolism of tumor cells, thereby modifying the response of these cells to drugs targeting metabolism. Drugs capable of inhibiting tumor proliferation may then become ineffective. Therefore, knowledge of microenvironmental nutrient levels is essential to a better understanding of tumor metabolism.

Outcomes for cancer patients vary greatly. The classification of BC into subtypes has been was defined in the literature on the basis of molecular characterization of proteomics (single omic). This has helped improve prognosis and personalized treatment. These considerations have motivated efforts to produce large amounts of multi-omic data such as TCGA [93] and ICGC [94]. However, current algorithms still face challenges and need to integrate omic data [95–98]. Defining BC subtypes using multi-omic data could help to better understand some of the dark areas that still persist in the field of tumor mechanisms in order to offer even more personalized treatments.

5. Conclusion

In the era of personalized medicine, OMICS science (genomics, transcriptomics, proteomics, and metabolomics) must contribute to the quest for cancer-specific biomarkers. The present study argues in favor of further research in this domain. Metabolomics is emerging as a relevant and promising tool for the classification of BC to enable more precise diagnosis [54,99–101]. Even though it is less accurate than the targeted approach, untargeted metabolomics nevertheless permits identification and quantification of a vast number of major metabolites. Thus, this approach presents a particular interest in the search for new candidate biomarkers [102–104] and could be applied in everyday medical practice given that the cost and duration of metabolomic analyses are relatively low. However, due to the retrospective design of our study and the small number of patients recruited, our results need to be validated in a larger cohort and in the context of a prospective clinical trial.

Funding

The authors declare no competing financial interests.

CrediT authorship contribution statement

Jocelyn Gal: Methodology, Formal analysis, Writing - original draft. **Caroline Bailleux:** Writing - original draft. **David Chardin:** Software, Writing - original draft. **Thierry Pourcher:** Conceptualization, Writing - review & editing. **Julia Gilhodes:** . **Lun Jing:** . **Jean-Marie Guigonis:** Methodology, Writing - review & editing. **Jean-Marc Ferrero:** Data curation. **Gerard Milano:** Writing - review & editing. **Baharia Mograbi:** Writing - review & editing. **Patrick Brest:** Writing - review & editing. **Yann Chateau:** . **Olivier Humbert:** Conceptualization, Writing - review & editing. **Emmanuel Chamorey:** Supervision, Methodology, Writing - review & editing.

Declaration of Competing Interest

The authors declare that they have no known competing financial interests or personal relationships that could have appeared to influence the work reported in this paper.

Acknowledgements

The authors acknowledge support from the Centre Antoine Lacassagne, TIRO Unit, University Côte d'Azur and the Departmental Council of the Alpes Maritimes, France.

The authors sincerely thank Mrs. Clair Della Vedova for her help in developing the figures.

Appendix A. Supplementary data

Supplementary data to this article can be found online at https://doi.org/10.1016/j.csbj.2020.05.021.

References

[1] Siegel RL, Miller KD, Jemal A. Cancer statistics, 2017. CA Cancer J Clin 2017;67:7–30.

[2] Perou CM, Jeffrey SS, van de Rijn M, et al. Distinctive gene expression patterns in human mammary epithelial cells and breast cancers. Proc Natl Acad Sci USA 1999;96:9212–7.

[3] Lockhart DJ, Winzeler EA. Genomics, gene expression and DNA arrays. Nature 2000;405:827–36.

[4] Pandey A, Mann M. Proteomics to study genes and genomes. Nature 2000;405:837–46.

[5] Perou CM, Sorlie T, Eisen MB, et al. Molecular portraits of human breast tumours. Nature 2000;406:747–52.

[6] Sorlie T, Perou CM, Tibshirani R, et al. Gene expression patterns of breast carcinomas distinguish tumor subclasses with clinical implications. Proc Natl Acad Sci U S A 2001;98:10869–74.

[7] Sorlie T, Tibshirani R, Parker J, et al. Repeated observation of breast tumor subtypes in independent gene expression data sets. Proc Natl Acad Sci USA 2003;100:8418–23.

[8] Witten DM, Tibshirani R. A framework for feature selection in clustering. J Am Stat Assoc 2010;105:713–26.

[9] Candido Dos Reis FJ, Wishart GC, Dicks EM, et al. An updated PREDICT breast cancer prognostication and treatment benefit prediction model with independent validation. Breast Cancer Res 2017;19:58.

[10] Wishart GC, Azzato EM, Greenberg DC, et al. PREDICT: a new UK prognostic model that predicts survival following surgery for invasive breast cancer. Breast Cancer Res 2010;12:R1.

[11] Ross JS. Multigene predictors in early-stage breast cancer: moving in or moving out?. Expert Rev Mol Diagn 2008;8:129–35.

[12] Ross JS, Hatzis C, Symmans WF, et al. Commercialized multigene predictors of clinical outcome for breast cancer. Oncologist 2008;13:477–93.

[13] Buyse M, Loi S, van't Veer L,, et al. Validation and clinical utility of a 70-gene prognostic signature for women with node-negative breast cancer. J Natl Cancer Inst 2006;98:1183–92.

[14] Cao Y, DePinho RA, Ernst M, Vousden K. Cancer research: past, present and future. Nat Rev Cancer 2011;11:749–54.

[15] Ehmann F, Caneva L, Prasad K, et al. Pharmacogenomic information in drug labels: European Medicines Agency perspective. Pharmacogenomics J 2015;15:201–10.

[16] McShane LM, Polley MY. Development of omics-based clinical tests for prognosis and therapy selection: the challenge of achieving statistical robustness and clinical utility. Clin Trials 2013;10:653–65.

[17] van de Vijver MJ, He YD, van't Veer LJ, et al. A gene-expression signature as a predictor of survival in breast cancer. N Engl J Med 2002;347:1999–2009.

[18] Wang Y, Klijn JG, Zhang Y, et al. Gene-expression profiles to predict distant metastasis of lymph-node-negative primary breast cancer. Lancet 2005;365:671–9.

[19] Wesolowski R, Ramaswamy B. Gene expression profiling: changing face of breast cancer classification and management. Gene Expr 2011;15:105–15.

[20] Marusyk A, Almendro V, Polyak K. Intra-tumour heterogeneity: a looking glass for cancer?. Nat Rev Cancer 2012;12:323–34.

[21] Hsu PP, Sabatini DM. Cancer cell metabolism: Warburg and beyond. Cell 2008;134:703–7.

[22] McClellan J, King MC. Genetic heterogeneity in human disease. Cell 2010;141:210–7.

[23] Cannon WB. The wisdom of the body. 2nd ed. Oxford, England: Norton & Co.; 1939.

[24] Roberts LD, Souza AL, Gerszten RE, Clish CB. Targeted metabolomics. Curr Protoc Mol Biol 2012. Chapter 30: Unit 30 32 31-24.

[25] Schrimpe-Rutledge AC, Codreanu SG, Sherrod SD, McLean JA. Untargeted metabolomics strategies-challenges and emerging directions. J Am Soc Mass Spectrom 2016;27:1897–905.

[26] Vinayavekhin N, Saghatelian A. Untargeted metabolomics. Curr Protoc Mol Biol 2010. Chapter 30: Unit 30 31 31-24.

[27] Camacho DM, Collins KM, Powers RK, et al. Next-generation machine learning for biological networks. Cell 2018;173:1581–92.

[28] Gal J, Milano G, Ferrero JM, et al. Optimizing drug development in oncology by clinical trial simulation: why and how? Brief Bioinform 2017.

[29] Yu MK, Ma J, Fisher J, et al. Visible machine learning for biomedicine. Cell 2018;173:1562–5.

[30] Jordan MI, Mitchell TM. Machine learning: trends, perspectives, and prospects. Science 2015;349:255–60.

[31] Tang P, Tse GM. Immunohistochemical surrogates for molecular classification of breast carcinoma: A 2015 update. Arch Pathol Lab Med 2016;140:806–14.

[32] Katajamaa M, Oresic M. Processing methods for differential analysis of LC/MS profile data. BMC Bioinf 2005;6:179.

[33] Pluskal T, Castillo S, Villar-Briones A, Oresic M. MZmine 2: modular framework for processing, visualizing, and analyzing mass spectrometry-based molecular profile data. BMC Bioinf 2010;11:395.

[34] Xia J, Mandal R, Sinelnikov IV, et al. MetaboAnalyst 2.0 – a comprehensive server for metabolomic data analysis. Nucleic Acids Res 2012;40:W127–133.

[35] Irizarry RA, Wang C, Zhou Y, Speed TP. Gene set enrichment analysis made simple. Stat Methods Med Res 2009;18:565–75.

[36] Saxena A, Prasad M, Gupta A, et al. A review of clustering techniques and developments. Neurocomputing 2017;267:664–81.

[37] Tibshirani R, Walther G, Hastie T. Estimating the number of clusters in a data set via the gap statistic. J Royal Stat Soc: Series B (Statistical Methodol) 2001;63:411–23.

[38] Kaufman L, Rousseeuw PJ. Finding groups in data: an introduction to cluster analysis. John Wiley & Sons; 2009.

[39] Rousseeuw PJ. Silhouettes: a graphical aid to the interpretation and validation of cluster analysis. J Comput Appl Math 1987;20:53–65.

[40] Davies DL, Bouldin DW. A cluster separation measure. IEEE Trans Pattern Anal Mach Intell 1979:224–7.

[41] Caliński T, Harabasz J. A dendrite method for cluster analysis. Commun Stat-Theory Methods 1974;3:1–27.

[42] Wang B, Zhu J, Pierson E, et al. Visualization and analysis of single-cell RNA-seq data by kernel-based similarity learning. Nat Methods 2017;14:414–6.

[43] Arthur D, Vassilvitskii S. k-means++: The advantages of careful seeding. In: Proceedings of the eighteenth annual ACM-SIAM symposium on Discrete algorithms. Society for Industrial and Applied Mathematics; 2007. p. 1027–35.

[44] Lloyd S. Least squares quantization in PCM. IEEE Trans. Inform. Theory 1982;28(2):129–37. https://doi.org/10.1109/TIT.1982.1056489.

[45] Steinhaus H. Sur la division des corps materiels en parties. Bull. Acad. Polon. Sci., C1. III 1956;IV:801–4.

[46] Ng AY, Jordan MI, Weiss Y. Analysis and an algorithm. In: Advances in neural information processing systems. On spectral clustering; 2002. p. 849–56.

[47] Von Luxburg U. A tutorial on spectral clustering. Stat Comput 2007;17:395–416.

[48] Tibshirani R. Regression shrinkage and selection via the lasso. J Roy Stat Soc: Ser B (Methodol) 1996:267–88.

[49] Gilet C, Deprez M, Caillau J-B, Barlaud M. Clustering with feature selection using alternating minimization, Application to computational biology. arXiv preprint arXiv:1711.02974 2017.

[50] Lvd Maaten, Hinton G. Visualizing data using t-SNE. J Mach Learn Res 2008;9:2579–605.

[51] Team RCR. A language and environment for statistical. Computing 2013.

[52] Witten DM, Tibshirani R. sparcl: Perform sparse hierarchical clustering and sparse k-means clustering. R package version 2013;1.

[53] Wishart GC, Bajdik CD, Azzato EM, et al. A population-based validation of the prognostic model PREDICT for early breast cancer. Eur J Surg Oncol 2011;37:411–7.

[54] Beger RD. A review of applications of metabolomics in cancer. Metabolites 2013;3:552–74.

[55] Gunther UL. Metabolomics biomarkers for breast cancer. Pathobiology 2015;82:153–65.

[56] McCartney A, Vignoli A, Biganzoli L, et al. Metabolomics in breast cancer: a decade in review. Cancer Treat Rev 2018;67:88–96.

[57] Silva C, Perestrelo R, Silva P, et al. Breast cancer metabolomics: from analytical platforms to multivariate data analysis. A Review. Metabolites 2019:9.

[58] Asiago VM, Alvarado LZ, Shanaiah N, et al. Early detection of recurrent breast cancer using metabolite profiling. Cancer Res 2010;70:8309–18.

[59] Cardoso MR, Santos JC, Ribeiro ML, et al. A Metabolomic approach to predict breast cancer behavior and chemotherapy response. Int J Mol Sci 2018;19.

[60] Karim MR, Beyan O, Zappa A, et al. Deep learning-based clustering approaches for bioinformatics. Brief Bioinform 2020.

[61] Bianchini G, Balko JM, Mayer IA, et al. Triple-negative breast cancer: challenges and opportunities of a heterogeneous disease. Nat Rev Clin Oncol 2016;13:674–90.

[62] Mills MN, Yang GQ, Oliver DE, et al. Histologic heterogeneity of triple negative breast cancer: A national cancer centre database analysis. Eur J Cancer 2018;98:48–58.

[63] Belkacemi Y, Hanna NE, Besnard C, et al. Local and regional breast cancer recurrences: salvage therapy options in the new era of molecular subtypes. Front Oncol 2018;8:112.

[64] Buonaguro FM, Caposio P, Tornesello ML, et al. Cancer diagnostic and predictive biomarkers 2018. Biomed Res Int 2019;2019:3879015.

[65] Ponde NF, Zardavas D, Piccart M. Progress in adjuvant systemic therapy for breast cancer. Nat Rev Clin Oncol 2018.

[66] Senkus E, Kyriakides S, Ohno S, et al. Primary breast cancer: ESMO Clinical Practice Guidelines for diagnosis, treatment and follow-up. Ann Oncol 2015;26(Suppl 5):v8–30.

[67] Assi HA, Khoury KE, Dbouk H, et al. Epidemiology and prognosis of breast cancer in young women. J Thorac Dis 2013;5(Suppl 1):S2–8.

[68] Wang K, Zhu GQ, Shi Y, et al. Long-term survival differences between T1–2 invasive lobular breast cancer and corresponding ductal carcinoma after breast-conserving surgery: A propensity-scored matched longitudinal cohort study. Clin Breast Cancer 2019;19:e101–15.

[69] Wasif N, Maggard MA, Ko CY, Giuliano AE. Invasive lobular vs. ductal breast cancer: a stage-matched comparison of outcomes. Ann Surg Oncol 2010;17:1862–9.

[70] Yersal O, Barutca S. Biological subtypes of breast cancer: Prognostic and therapeutic implications. World J Clin Oncol 2014;5:412–24.

[71] Topol EJ. High-performance medicine: the convergence of human and artificial intelligence. Nat Med 2019;25:44–56.

[72] Pavlova NN, Thompson CB. The emerging hallmarks of cancer metabolism. Cell Metab 2016;23:27–47.

[73] Hainaut P, Plymoth A. Targeting the hallmarks of cancer: towards a rational approach to next-generation cancer therapy. Curr Opin Oncol 2013;25:50–1.

[74] Hanahan D, Weinberg RA. Hallmarks of cancer: the next generation. Cell 2011;144:646–74.

[75] Li Z, Zhang H. Reprogramming of glucose, fatty acid and amino acid metabolism for cancer progression. Cell Mol Life Sci 2016;73:377–92.

[76] DeBerardinis RJ, Chandel NS. Fundamentals of cancer metabolism. Sci Adv 2016;2:e1600200.

[77] Haukaas TH, Euceda LR, Giskeodegard GF, Bathen TF. Metabolic portraits of breast cancer by HR MAS MR spectroscopy of intact tissue samples. Metabolites 2017:7.

[78] Jeon H, Kim JH, Lee E, et al. Methionine deprivation suppresses triple-negative breast cancer metastasis in vitro and in vivo. Oncotarget 2016;7:67223–34.

[79] Melone MAB, Valentino A, Margarucci S, et al. The carnitine system and cancer metabolic plasticity. Cell Death Dis 2018;9:228.

[80] Thomas TJ, Thomas T. Cellular and animal model studies on the growth inhibitory effects of polyamine analogues on breast cancer. Med Sci (Basel) 2018:6.

[81] Xiao F, Wang C, Yin H, et al. Leucine deprivation inhibits proliferation and induces apoptosis of human breast cancer cells via fatty acid synthase. Oncotarget 2016;7:63679–89.

[82] Zuo Y, Ulu A, Chang JT, Frost JA. Contributions of the RhoA guanine nucleotide exchange factor Net1 to polyoma middle T antigen-mediated mammary gland tumorigenesis and metastasis. Breast Cancer Res 2018;20:41.

[83] Lecuyer L, Dalle C, Lyan B, et al. Plasma metabolomic signatures associated with long-term breast cancer risk in the SU.VI.MAX prospective cohort. Cancer Epidemiol Biomarkers Prev 2019.

[84] Oikari S, Kettunen T, Tiainen S, et al. UDP-sugar accumulation drives hyaluronan synthesis in breast cancer. Matrix Biol 2018;67:63–74.

[85] Pan H, Xia K, Zhou W, et al. Low serum creatine kinase levels in breast cancer patients: a case-control study. PLoS One 2013;8:e62112.

[86] Phannasil P, Ansari IH, El Azzouny M, et al. Mass spectrometry analysis shows the biosynthetic pathways supported by pyruvate carboxylase in highly invasive breast cancer cells. Biochim Biophys Acta Mol Basis Dis 2017;1863:537–51.

[87] Mason EF, Rathmell JC. Cell metabolism: an essential link between cell growth and apoptosis. Biochim Biophys Acta 2011;1813:645–54.

[88] Hensley CT, Wasti AT, DeBerardinis RJ. Glutamine and cancer: cell biology, physiology, and clinical opportunities. J Clin Invest 2013;123:3678–84.

[89] Warburg O, Wind F, Negelein E. The metabolism of tumors in the body. J Gen Physiol 1927;8:519–30.

[90] Anderson NM, Mucka P, Kern JG, Feng H. The emerging role and targetability of the TCA cycle in cancer metabolism. Protein Cell 2018;9:216–37.

[91] Fernandez MF, Reina-Perez I, Astorga JM, et al. Breast Cancer and Its Relationship with the Microbiota. Int J Environ Res Public Health 2018;15.

[92] Sullivan MR, Danai LV, Lewis CA, et al. Quantification of microenvironmental metabolites in murine cancers reveals determinants of tumor nutrient availability. Elife 2019:8.

[93] Cancer Genome Atlas Research N. Comprehensive genomic characterization defines human glioblastoma genes and core pathways. Nature 2008;455:1061–8.

[94] Zhang J, Baran J, Cros A, et al. International Cancer Genome Consortium Data Portal–a one-stop shop for cancer genomics data. Database (Oxford) 2011;2011:bar026.

[95] Mitra S, Saha S. A multiobjective multi-view cluster ensemble technique: Application in patient subclassification. PLoS One 2019;14:e0216904.

[96] Ramazzotti D, Lal A, Wang B, et al. Multi-omic tumor data reveal diversity of molecular mechanisms that correlate with survival. Nat Commun 2018;9:4453.

[97] Rappoport N, Shamir R. Multi-omic and multi-view clustering algorithms: review and cancer benchmark. Nucleic Acids Res 2018;46:10546–62.

[98] Wu C, Zhou F, Ren J, et al. A selective review of multi-level omics data integration using variable selection. High Throughput 2019:8.

[99] Armitage EG, Barbas C. Metabolomics in cancer biomarker discovery: current trends and future perspectives. J Pharm Biomed Anal 2014;87:1–11.

[100] Bennett DA, Waters MD. Applying biomarker research. Environ Health Perspect 2000;108:907–10.

[101] Vermeersch KA, Styczynski MP. Applications of metabolomics in cancer research. J Carcinog 2013;12:9.

[102] Jacob M, Lopata AL, Dasouki M, Abdel Rahman AM. Metabolomics toward personalized medicine. Mass Spectrom Rev 2017.

[103] Trivedi DK, Hollywood KA, Goodacre R. Metabolomics for the masses: The future of metabolomics in a personalized world. New Horiz Transl Med 2017;3:294–305.

[104] Wishart DS. Emerging applications of metabolomics in drug discovery and precision medicine. Nat Rev Drug Discov 2016;15:473–84.